

## Free-energy calculations in structure-based drug design

Michael R. Shirts, David L. Mobley, and Scott P. Brown

### INTRODUCTION

The ultimate goal of structure-based drug design is a simple, robust process that starts with a high-resolution crystal structure of a validated biological macromolecular target and reliably generates an easily synthesized, high-affinity small molecule with desirable pharmacological properties. Although pharmaceutical science has made significant gains in understanding how to generate, test, and validate small molecules for specific biochemical activity, such a complete process does not now exist. In any drug design project, enormous amounts of luck, intuition, and trial and error are still necessary.

For any small molecule to be considered a likely drug candidate, it must satisfy a number of different absorption/distribution/metabolism/excretion (ADME) properties and have a good toxicological profile. However, a small molecule must above all be active, which in most cases means that it must bind tightly and selectively to a specific location in the protein target before any of the other important characteristics are relevant. To design a drug, large regions of chemical space must be explored to find candidate molecules with the desired biological activity. High-throughput experimental screening methods have become the workhorse for finding such hits.<sup>1,2</sup> However, their results are limited by the quality and diversity of the preexisting chemical libraries, which may contain only molecules representative of a limited portion of the relevant chemical space for a given target. Combinatorial libraries can be produced to supplement these efforts, but their use requires careful design strategies and they are subject to a number of pitfalls.<sup>3</sup> More focused direct *in vivo* or *in vitro* measurements provide important information about the effect of prospective drugs in the complete biological system but provide relatively little information that can be directly used to further engineer new molecules. Given a small number of molecules, highly accurate assays of binding, such as surface plasmon resonance (SPR) or isothermal calorimetry (ITC), are relatively accessible though rather costly.

Ideally, small molecules with high potential biological activity could be accurately and reliably screened by computer before ever being synthesized. The degree of accuracy

that is required of any computational method will depend greatly its speed. A number of rapid structure-based virtual screening methods, generally categorized as “docking,” can help screen large molecular libraries for potential binders and locate a putative binding site (see Chapter 7 for more information on docking). However, recent studies have illustrated that although docking methods can be useful for identifying putative binding sites and identifying ligand poses, scoring methods are not reliable for predicting compound binding affinities and do not currently possess the accuracy necessary for lead optimization.<sup>4-6</sup>

Atomistic, physics-based computational methods are appealing because of their potential for high transferability and therefore greater reliability than methods based on informatics or extensive parameterization. Given a sufficiently accurate physical model of a protein/ligand complex and thorough sampling of the conformational states of this system, one can obtain accurate predictions of binding affinities that could then be robustly incorporated into research decisions. By using a fundamental physical description, such methods are likely to be valid for any given biological system under study, as long as sufficient physical detail is included. Yet another advantage of physics-based models is that the failures can be more easily recognized and understood in the context of the physical chemistry of the system, which cannot be easily done in informatics-based methods.

Despite this potential for reliable predictive power, few articles exist in the literature that report successful, prospective use of physics-based tools within industrial or academic pharmaceutical research. Some of the likely reasons for such failures are the very high computational costs of such methods, insufficiently accurate atomistic models, and software implementations that make it difficult for even experts to easily set up with each new project. Until these problems are resolved, there remain significant obstacles to the realization of more rigorous approaches in industrial drug research.

There have been a number of important technical advances in the computation of free energies since the late 1990s that, coupled with the rapid increase in computational power, have brought these calculations closer to

the goal of obtaining reliable and pharmaceutically useful binding energies. In this chapter, we briefly review these latest advances, with a focus on specific applications of these methods in the recent literature. Under “How Accurate Must Calculations of Affinity Be to Add Value” we first discuss the level of reliability and accuracy that binding calculations must have to add some degree of value to the pharmaceutical process. Under “Free Energy Methodologies” we give an overview of the methods currently used to calculate free energies, including recent advances that may eventually lead to sufficiently high throughput for effective pharmaceutical utility. Under “MM-PBSA Calculations” and “Alchemical Calculations” we review recent ligand binding calculations in the literature, beginning with relatively computationally efficient methods that are generally more approximate but still attempt to calculate a true affinity without system-dependent parameters and then address pharmaceutically relevant examples of most physically rigorous methods. We conclude with a discussion of the implications of recent progress in calculating ligand binding affinities on structure-based drug design.

#### HOW ACCURATE MUST CALCULATIONS OF AFFINITY BE TO ADD VALUE?

Physics-based binding calculations can be very computationally demanding. Given these time requirements, it is important to understand quantitatively what levels of precision, throughput, and turnaround time are required for any computational method to systematically effect the lead-optimization efforts of industrial medicinal chemists in a typical work flow. To be useful, a method does not necessarily need to deliver perfect results, as long as it can produce reliable results with some predictive capacity on time scales relevant to research decision-making processes. These issues are frequently addressed anecdotally, but rarely in a quantitative manner, and we will try to sketch out at least one illustration of what the requirements of a computational method might be.

A recent analysis of more than 50,000 small-molecule chemical transformations spanning over 30 protein targets at Abbott Laboratories found that approximately 80% of the resulting modified molecules had potencies lying within 1.4 kcal/mol (i.e., 1  $pK_i$  log unit) of the starting compound.<sup>7</sup> Potency gains greater than 1.4 kcal/mol from the parent were found to occur approximately 8.5% of the time, whereas gains in potency greater than 2.8 kcal/mol were found with only 1% occurrence. Losses in binding affinity on modification were approximately equal in magnitude and probability to the gains for most types of modifications; presumably wholly random chemical changes would result in a distribution with losses in binding that are much more common than gains. We treat this distribution as typical of lead-optimization affinity gains obtained by skilled medicinal chemists and use this distribution to examine the

ability of accurate and reliable computational methods to influence drug research productivity.

Suppose our chemist sits down each week and envisions a large number of modifications of a lead compound he or she would like to make and test. Instead of simply selecting only his or her best guess from that list, which would lead to a distribution in affinity gains similar to the one described above, this chemist selects  $N$  compounds to submit to an idealized computer screening program. The chemist then synthesizes the top-rated compound from the computer predictions. What is the expected distribution of affinities arising from this process for different levels of computational error?

To model this process, we assume the medicinal chemist's proposals are similar to the Abbott data and we approximate this distribution of binding affinity changes as a Gaussian distribution with mean zero and standard deviation of 1.02 kcal/mol, resulting in 8.5% of changes having a  $pK_i$  increase of 1.0. We assume the computational predictions of binding affinity have Gaussian noise with standard deviation  $\epsilon$ . In our thought experiment, we generate  $N$  “true” binding affinity changes from the distribution. The computational screen adds Gaussian error with width  $\epsilon$  to each measurement. We then rank the “noisy” computational estimates and look at distribution of “true” affinities that emerge from selecting the best of the corresponding “noisy” estimates. Repeating this process a number of times (for Figure 5.1, one million), we can generate a distribution of affinities from the screened process.

Shown in Figure 5.1 is the modeled distribution of experimental affinity changes from the chemist's predictions (blue) versus the distribution of the experimental affinity changes after computationally screening  $N = 10$  compounds with noise  $\epsilon = 0.5$  (pink),  $\epsilon = 1.0$  (red), and  $\epsilon = 2.0$  (purple). In other words, the blue distribution of affinities is what the medicinal chemist would obtain alone; the redder curves what the chemist would obtain synthesizing the computer's choice of his  $N$  proposed modification. The shaded area represents the total probability of a modification with affinity gain greater than 1.4 kcal/mol.

With 0.5 kcal/mol computational noise, screening just ten molecules results in an almost 50% chance of achieving 1  $pK_i$  binding increase in a single round of synthesis, versus an 8.5% chance without screening. With 1 kcal/mol error, we still have 36% chance of achieving this binding goal with the first molecule synthesized. Surprisingly, even with 2 kcal/mol, computational noise almost triples the chance of obtaining a 1  $pK_i$  binding increase. Similar computations can be done with large numbers of computer evaluations; unsurprisingly, the more computational evaluations can be done, the more computational noise can be tolerated and still yield useful time savings. For example, even with 2 kcal/mol error, screening 100 molecules results in the same chance of producing a 1  $pK_i$  binding increase that is the same as if ten molecules are screened with 0.5 kcal/mol error.

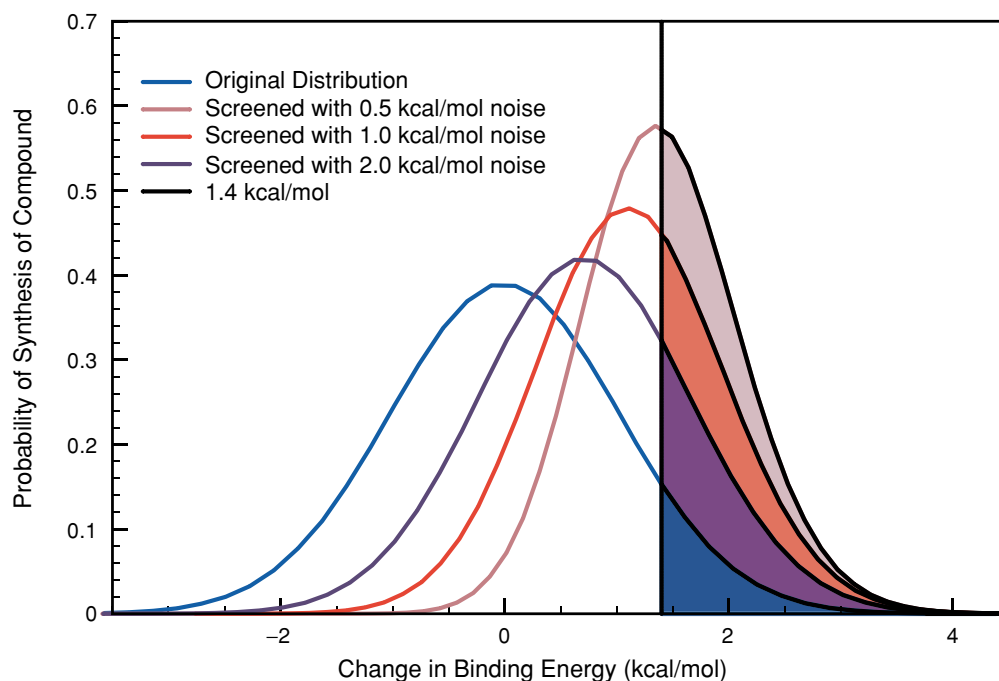


**Figure 5.1.** Modeled distribution of affinity changes of the proposed modifications (blue) compared to the distribution of affinity changes after computational screening with Gaussian error  $\epsilon = 0.5$  (pink),  $\epsilon = 1.0$  (red), and  $\epsilon = 2.0$  (purple). The shaded area represents the total probability of a proposed modification with affinity gain greater than 1.4 kcal/mol. Hence, in many situations, even with moderate error, a reliable method of filtering compounds could significantly improve the efficiency of synthesis in lead optimization.

So even relatively small numbers of moderately accurate computer predictions may be able to give significant advantage in the pharmaceutical work flow. When we translate the chance of obtaining binding improvement into the number of rounds of synthesis required to obtain that improvement, then screening 100 molecules with 2 kcal/mol noise or 10 screened molecules with 0.5 kcal/mol noise in this model reduces the number of molecules to be synthesized by almost an order of magnitude. Clearly, these calculations assume the simulations are not biased against active compounds, and errors that are highly dependent on the binding system would result in less reliable advantages. The type of computation matters as well – computing relative binding affinities would require only one calculation to compare affinity changes, whereas absolute binding affinities would require two, increasing the effective error. But physically based prediction methods should in principle be more reliable than parameterized methods, as the basic physics and the atomistic details are transferable between drug targets.

This analysis is in agreement with informal discussions with pharmaceutical chemists, who mentioned reliability as being more important than pure speed or the highest accuracy. Many thought they could fit methods that took as much as a month into a work flow, as long as they truly converged reliably with 1 kcal/mol variance error. Even a slight decrease in reliability, for example, being off by several kcal/mol more than 20% of the time, greatly decreased the

amount of time that scientists would be willing to wait, perhaps down to a day or two.

## FREE-ENERGY METHODOLOGIES

A very large number of methods for computing binding free energies with atomistic molecular models have been developed. Most of them are still under active study, and each has different trade-offs between accuracy and computational efficiency. Because of the scale, complexity, and speed of methodological developments, choosing and applying methods can be confusing even to experienced practitioners. Here, we focus on an overview of some of the key methods available for computing binding affinities, emphasizing references to primary literature. A number of useful recent reviews have focused specifically on free energy methods.<sup>8–14</sup> Of particular note is a recent, fairly comprehensive book on free-energy methods, specifically Chapters 1–7.<sup>15</sup> Several molecular simulation and modeling textbooks have useful introductions to free-energy calculations as well.<sup>16–18</sup>

In this discussion of methods, we will assume standard classical molecular mechanics models, with harmonic bond and angle terms, periodic dihedral terms, and non-bonded terms consisting of point charges and Lennard–Jones repulsion/dispersion terms. In the vast majority of ligand-binding free-energy methods, calculations have been performed with these types of models. Adding

classical polarizability terms has seldom been done, though we will briefly mention attempts to include these. Computing free energies using mixed QM/MM simulations can be done but its use has been even more restricted and so will not be discussed here.<sup>19</sup>

### Basic equations

The binding affinity  $K_d$  of a small molecule ligand  $L$  to a protein  $P$  can be expressed simply by

$$K_d = \frac{[L][P]}{[PL]}, \quad (5.1)$$

where the brackets denote an equilibrium concentration,  $L$  is the ligand,  $P$  is the protein, and  $PL$  is the protein/ligand complex. This definition makes the assumption that the difference between bound and unbound states can be well defined, an assumption that is essentially always valid for tight, specific binders but becomes more complicated for very weak and nonspecific binders.

This binding affinity can then be related to the free energy of binding by

$$\Delta G_{\text{Bind}} = -kT \ln \frac{K_d}{C^\circ}, \quad (5.2)$$

where  $C^\circ$  indicates the standard state concentration (by convention, 1 M for solutions). We use the Gibbs free energy  $G$  in our equations, because situations of pharmaceutical interest are usually under constant pressure.

The free energy of binding can also be expressed as

$$\Delta G_{\text{Bind}} = -kT \ln \frac{Z_P Z_L}{C^\circ Z_{PL}}, \quad (5.3)$$

where  $Z$  represents the partition function of the system. It is this quantity that we wish to calculate via simulation.

### MM-PBSA

As a compromise between speed and accuracy for physics-based estimates of protein/ligand binding affinities, we first discuss the end-point free-energy method molecular mechanics with Poisson–Boltzmann and surface area (MM-PBSA).<sup>20</sup> As an end-point method, MM-PBSA requires direct simulation of only the bound and unbound states. This simplification comes with the expectation of significantly larger intrinsic errors with MM-PBSA than with other more rigorous methods we will address later in the chapter.

The free energy of binding can be written as a difference in the solvation free energies of each of the components:

$$\Delta G_{\text{Bind}} = \Delta G_{\text{PL-solv}} - \Delta G_{\text{L-solv}} + \Delta G_{\text{P-solv}}. \quad (5.4)$$

Each of these solvation energies can be written as

$$\Delta G_{\text{solv}} = \Delta H_{\text{solv}} - T\Delta S_{\text{solv}}. \quad (5.5)$$

If we average out the coordinates of the solvent over all the configurations, then we can approximate each of these free energies as

$$\Delta G_{X-\text{solv}} = \langle E_X \rangle + \Delta G_{X-\text{solvent}} - T\Delta S_{X-\text{MM}}, \quad (5.6)$$

where  $\langle E_X \rangle$  is the average molecular mechanics energy of  $X$  alone (without water),  $\Delta S_X$  is the internal entropy of

$X$  (without water), and  $\Delta G_{X-\text{solvent}}$  is the energy and entropy due to the solvation of  $X$  waters. These solvation energies for  $P$ ,  $L$ , and  $PL$  can then be combined to compute a full binding energy.

In practice, a variety of implementations of the MM-PBSA protocol have been reported, and particular care needs to be paid to a number of details in setting up the calculations. In general, protocols can be separated into three steps. First, coordinate sampling [such as molecular dynamics (MD)] is performed on the protein/ligand complex to sample configurations for energy analysis. In the next step, calculation of gas-phase potential energies and solvation free energies is performed on each structure collected from the previous step to produce ensemble averages. Finally, some measure of estimated change in solute entropy is computed for the set of structures. The final binding free energy is then obtained by combining these various components.

To generate the structures in the first step, one can perform separate MD simulations for the isolated ligand, apo protein, and bound protein/ligand complex. Alternatively, one can use a single trajectory of the bound complex as the source of conformations for the unbound (and bound) states.<sup>21</sup> This second case is equivalent to assuming that the conformations explored in the protein/ligand complex in solution are sufficiently similar to those conformations explored by the apo protein and isolated ligand. This assumption is not necessarily reasonable and in fact is guaranteed to be grossly incorrect in some contexts; however, the amount of noise added when taking differences between averages produced from independent bound and unbound trajectories substantially increases the sampling required for convergence, so by simulating one structure, lower variance is traded for some bias.<sup>22,23</sup> In theory, one could then perform a single MD run of the apo protein, and all additional runs would involve only isolated ligands. In any case, determining arrival at a stable average can be challenging.<sup>24</sup> A possible alternative formulation for the case of running the three separate trajectories is to disregard all energies but the interaction energies in an attempt to dampen the contributions to noise due to noncanceling internal-energy differences.

The potential energy  $E_{X-\text{MM}}$  is that of only the protein and ligand and consists of

$$E_{X-\text{MM}} = E^{\text{elec}} + E^{\text{vdW}} + E^{\text{int}}, \quad (5.7)$$

where  $E^{\text{elec}}$  is the electrostatic energy,  $E^{\text{vdW}}$  is the van der Waals dispersion and repulsion, and  $E^{\text{int}}$  is composed of internal-energy terms for the ligand and protein, such as bond, angle, and torsion terms.

The solvation energy term  $\Delta G_{X-\text{solvent}}$  is subdivided into a sum of two components, one due to electrostatic interaction and the other due to nonpolar interactions:

$$\Delta G_{X-\text{solvent}} = \Delta G_{\text{PBSA}} = \Delta G_{\text{PB}} + \Delta G_{\text{SA}}, \quad (5.8)$$

where  $\Delta G_{\text{PB}}$  represents the polar contribution and  $\Delta G_{\text{SA}}$  represents the nonpolar contribution to the solvation free energy.

The polar term in Equation (5.8) represents the energy stored in the continuum dielectric in response to the presence of the solute's charge distribution and is typically obtained by solution of the Poisson–Boltzmann (PB) equation. The PB equation provides a rigorous framework for representing discrete solute molecules embedded in a uniform dielectric continuum and has been shown to be capable of producing relatively robust predictions of electrostatic contributions to solvation free energies of small molecules as well as biological macromolecules.<sup>25,26</sup> The PB solutions are obtained in separate calculations for the ligand, protein, and bound protein/ligand complex, and the final solvation free-energy values are assembled using the thermodynamic cycle for association in solution.<sup>27,28</sup>

For any PB calculation, one must choose a particular representation of the dielectric boundary between solute and solvent, which can involve a number of subtleties.<sup>29,30</sup> In addition to the boundary representation, dielectric functions for the solute and solvent must also be chosen. For typical protein/ligand systems, constant values of 1.0 for solutes and 80.0 for solvent are most commonly used,<sup>31</sup> though there are also other arguments that using 2.0, 4.0, or a residue-based dielectric for the solute may give superior performance.<sup>32,33</sup> It should be noted that most force fields have been parameterized using an internal dielectric of 1.0.

Finally, the last term in Equation (5.8) is the nonpolar component of solvation free energy, which is usually treated as being proportional to the solvent exposed surface area<sup>34</sup> of the solute,

$$G^{\text{SA}} = \gamma \Delta SA, \quad (5.9)$$

where  $\Delta SA$  is the change in accessible molecular surface area on binding, and  $\gamma$  is a microscopic surface free energy for formation of a cavity in water.<sup>35</sup> The form of this equation derives from empirical data on transfer free energies for linear, cyclic, and branched hydrocarbons.<sup>36,37</sup> The precise value of  $\gamma$  depends on the particular method used to probe the solvent-accessible surface of the solute.<sup>25</sup> The equation implicitly assumes that the nonpolar component has negligible contributions from dispersion interactions between solute and solvent relative to the energy required in displacing solvent molecules to create the cavity. A number of objections to this expression point out its oversimplification,<sup>38–40</sup> and a number of models have been proposed to attempt to address these shortcomings with more sophisticated frameworks.<sup>39–41</sup>

The last term on the right-hand side of Equation (5.6) is the entropic cost of confining the free ligand, which represents a significant fraction of the total change in solute entropy  $\Delta S_{\text{solute}}$  for formation of the bound complex. Additional estimates of solute entropy can be performed, which typically use some form of normal-mode analysis and that are very computationally expensive to perform.<sup>42,43</sup> Alterna-

tively, one could use empirical estimates of average entropic costs, such as the entropy required to constrain rotation around any given torsional degree of freedom.<sup>44</sup> However, neither of these approaches produce quality estimates of solute entropy; instead, they tend to add a significant random scatter to results.<sup>21</sup>

Because of the complications in dealing with entropy, it is often neglected for computational convenience. This approximation may be reasonable in cases where we are only interested in rank-ordering, and the amount of entropy/enthalpy compensation remains roughly constant across ligands. It will certainly be unreasonable for any case where absolute comparisons of free energy are desired across protein targets and in situations for which non-negligible perturbations in binding modes and pocket geometries occur across a ligand set. Recent developments for treating the entropy more properly show significant promise.<sup>45</sup>

In systems where there are relatively few populated states, it may be sufficient to perform PB calculations alone to generate robust affinity estimates. In a number of situations, PB solutions have been successfully used to estimate affinities,<sup>28,46–48</sup> although some implementations begin to resemble empirical scoring methods.<sup>49</sup> A major criticism of these approaches is their potential inaccuracy in situations where conformational flexibility plays a significant role.<sup>50</sup>

In generating the dynamics trajectories for the MM-PBSA analysis explicit representation of water molecules are typically used. Although explicit water molecules give the most detailed glimpse into structural dynamics, it has been shown that there can be pathologies in certain situations when using implicit-solvent theory to “score” explicit water configurations,<sup>21,51</sup> because the ensemble average energies should be computed with the same energy function used to generate the ensemble structures. An alternative to this is to sample in implicit solvent directly.<sup>52</sup>

As PB solutions are in general computationally demanding calculations, a number of groups have put significant efforts into developing faster approximations, such as the suite of generalized Born (GB) approaches.<sup>53–56</sup> However, there are numerous examples of pathologies using GB methods.<sup>57–59</sup>

### Other implicit solvent methods

Another approach requiring only simulations of the bound and unbound states is to compute the partition function directly. The partition function of a molecular system can be computed as the sum of the integral of Boltzmann factors over neighborhoods of only the low-energy states, which are a relatively small fraction of the total configurations of the molecules.<sup>60</sup>

With the full partition function for the protein, ligand, and the complex in the case of absolute free energies, or for two ligands and two complexes in the case of relative free energies, the binding free energy or changes in binding

free energy can be computed directly from these end states. At least two methods for computing the configuration integrals in the neighborhood of minima have been developed that have been applied to ligand binding systems: mode integration (MINTA),<sup>61</sup> and the Mining Minima approaches of Gilson and coworkers. Both start out with a method for enumerating minima. In MINTA importance sampling Monte Carlo integration is used to calculate the configuration integrals. It has been used to screen for the free-energy difference between ligand enantiomers, where its accuracy was comparable to alchemical methods, but was more efficient,<sup>62,63</sup> though there are important caveats in the original implementation.<sup>64</sup> Gilson and coworkers have emphasized calculating the integrals in bond/angle/torsion coordinates to minimize errors.<sup>68</sup> They have applied such methods successfully to a number of simplified binding systems.<sup>65–68</sup>

The methods' two shared main problems are the need to find all minima contributing to the partition function and the correct computation of entropies of neighborhoods near minima. Minima searches of proteins the size of typical drug targets are notoriously difficult, and hence the studies noted above focus mostly on problems where many of the errors may cancel out or on smaller model systems. The problems of estimating entropy in these methods has much in common with the same problem in MM-PBSA calculations, though because these methods are perhaps more sensitive to the correct entropy calculation, the problems have been investigated to a significant degree.<sup>45,61,69,70</sup> However, significantly fewer people are investigating these alternative end-point methods than MM-PBSA, and they are generally more computationally expensive, so the short-term prospects are not necessarily particularly encouraging despite the strong theoretical underpinnings.

### Alchemical methods

The methods described above are designed primarily for implicit solvent systems and represent relatively computationally cheap approximations to the binding free energy. However, implicit water models are unsuitable for a fully molecular description of phenomena such as the formation of correlated hydrogen bonding networks in binding active sites and there are many protein/ligand systems where the atomic detail of the water in the binding site plays an important role in the binding process.<sup>71</sup> For free-energy calculations to include these phenomena, more expensive explicit water simulations must be used. Using explicit water, the free-energy terms in MM-PBSA become dominated by statistical noise from the water. The standard approach for solvation free energies in explicit solvent simulations is instead to compute the free energy of a particular change of state directly, while holding the rest of the system fixed, which does not depend directly on the energies of the rest of the system. We note that although these methods

are the techniques of choice for explicit water simulations, they can be performed equally easily for continuum water simulations.

“Free-energy perturbation” is a very common term for these methods that directly compute the free-energy difference as a function of changing molecular structure. “Perturbation” usually refers to an approximate theory that can be written as a series of more easily calculated terms. Free-energy perturbation (frequently abbreviated FEP), however, is exact. The term *perturbation* here instead refers to the changes in the chemical identity, as simulations frequently involve changes in chemical identity, such as an amine to an alcohol or a methyl group to a chlorine. Additionally, FEP is sometimes used to refer specifically to application of the Zwanzig relationship (discussed below). To avoid confusion, we will use the term *alchemical* to refer to this class of methods, as the chemical identity of the atomic models will change, appear, or disappear during the process, and use EXP to refer to the Zwanzig relationship.

### Zwanzig relationship

The most well-known method historically for calculating free energies, and still a very common one, is the Zwanzig relationship.<sup>72</sup> The free energy between two Hamiltonians  $H_0(x)$  and  $H_1(x)$  over a coordinate and momentum space  $(x)$  can be calculated as

$$\Delta G = \beta^{-1} \ln \langle e^{-\beta[H_1(x) - H_0(x)]} \rangle_0 = \beta^{-1} \ln \langle e^{-\beta \Delta H(x)} \rangle_0, \quad (5.10)$$

where  $\beta = (kT)^{-1}$ . We will denote this method EXP, for exponential averaging. Although the equation is exact, many studies have demonstrated that except in the case of rather small changes, EXP convergence as a function of the amount of data collected is far from ideal, and an average that appears to have converged may only indicate very poor overlap between the two states studied.<sup>73,74</sup>

Overlap in configuration space in the direction of decreasing entropy is usually greater, and thus EXP in this direction will generally be more efficient.<sup>75,76</sup> For example, inserting a molecule into a dense fluid is a more effective way to compute the chemical potential than deleting molecules from the same fluid, because the important conformations for both ensembles are actually easiest to sample in simulations without the molecule present.

### Multiple intermediates

In some cases, such as computing the chemical potential of bulk fluids, the symmetry of the problem can be used to greatly improve computational efficiency of FEP.<sup>77</sup> However, in most instances where the states of interest are very far from having any phase-space overlap, the transformation can be broken into a series of free-energy calculations with nonphysical intermediates – for example, turning off the atomic charges or turning a carbon into an oxygen. The

total free energy can simply be written as a sum of the individual free energies between intermediate states, which can be completely nonphysical. We will first assume the existence of these intermediates, and the ability to perform simulations at these intermediates and then discuss the best choice of intermediate states.

If phase-space overlap between consecutive intermediates is very high, then EXP can work well. For example, if an ether is changed to a thioether, there is relatively little change in phase-space, and EXP will be effective with a small number of intermediates. However, if an entire heavy atom is disappearing or appearing or if the charge of an atom is changing significantly, phase-space overlap will not be significant, and EXP is almost guaranteed to do poorly without a large number of intermediates. Because of the large number of intermediates required, computations with EXP can be very inefficient, requiring the simulation of many states for computing the free energy of a single alchemical transformation.

Double-wide sampling is a commonly used technique that consists of simulating only at every other intermediate state and computing EXP in both directions from these intermediates.<sup>78</sup> The biases of free energy computed from EXP in different directions have opposite signs, so alternating directions will tend to cancel bias somewhat. This method nominally reduces the number of simulations necessary by half, but because the variance in the direction of increasing entropy is usually lower, this twofold gain in efficiency is rarely obtained. Fortunately, there are a number of alternatives that are more efficient than EXP in most cases.

### Thermodynamic integration

By taking the derivative of the free energy with respect to some continuous parameter  $\lambda$  describing a series of intermediate alchemical states, we can see that

$$\begin{aligned} dG/d\lambda &= \frac{d}{d\lambda} \int e^{-\beta H(\lambda, \mathbf{x})} d\mathbf{x} = \left\langle \frac{dH(\lambda, \mathbf{x})}{d\lambda} \right\rangle_{\lambda} \\ \Delta G &= \int_0^1 \left\langle \frac{dH(\lambda, \mathbf{x})}{d\lambda} \right\rangle_{\lambda} d\lambda, \end{aligned} \quad (5.11)$$

where the pathway of intermediates between the states of interest is parameterized between  $\lambda = 0$  and  $\lambda = 1$ . This formula can also be obtained by expanding the Zwanzig relationship in a Taylor series. Computing free energies using this formula is typically called thermodynamic integration (TI). In the rest of the discussion, we will denote  $H(\lambda, \mathbf{x})$  by simply  $H(\lambda)$ . Note that when the end states have different masses, the momenta will have  $\lambda$  dependence as well, which must also be included in the derivative, but we omit this detail for clarity in the discussion.

Thermodynamic integration essentially trades variance for bias. Averaging over  $\left\langle \frac{dH}{d\lambda} \right\rangle$  will require fewer uncorrelated samples to reach a given level of relative error than averaging  $e^{-\beta \Delta H(\lambda)}$ , as long as  $\left\langle \frac{dH}{d\lambda} \right\rangle$  is well behaved, an important condition we will address later in the section “Choice of

Alchemical Pathways.” However, to compute the total free energy from a series of individual simulations, we must use some type of numerical integration of the integral, which by definition introduces bias. A number of different numerical techniques have been applied.<sup>79,80</sup> A simple trapezoidal rule is usually used or, occasionally, Simpson’s rule. Higher order integration methods converge more quickly in the distance between integration points, but this error term is proportional to the derivatives of the function, which can become large in some situations, such as when repulsive atomic centers are removed from the system entirely. Other techniques such as Gaussian integration have been used<sup>79</sup> but require knowledge about the variance to determine the Gaussian weighting and so become cumbersome to use.

For alchemical changes that result in smooth, monotonic curves for  $\langle dH/d\lambda \rangle$ , TI can be quite accurate using a relatively small number of points. However, if the curvature becomes large, as can frequently be the case in alchemical simulations where Lennard–Jones potentials are turned on or off, then the bias introduced by discretization of the integral can become large.<sup>73,81,82</sup> Even in the case of small curvature (i.e., charging of SPC water in water) reasonably large errors can be introduced (i.e., 5–10% of the total free energy with 5  $\lambda$  values).<sup>83</sup>

Many early free-energy calculations approximated the integral by varying  $\lambda$  throughout the simulation, called “slow growth.” The total free energy is then estimated as

$$\Delta G \approx \int_{t=t_0}^{t_1} \left\langle \frac{dH}{d\lambda} \right\rangle_{\lambda(t)} \frac{d\lambda}{dt} dt. \quad (5.12)$$

This, however, proved to be a very bad approximation in most molecular simulations, introducing large speed-dependent biases even for relatively long simulations. Forward and reverse simulations show significant hysteresis.<sup>84,85</sup> This method should always be avoided, except when used in the context of Jarzynski’s relationship, which we will now discuss.

### Jarzynski’s relationship

If we have a physical or alchemical process that takes place in finite time, the amount of work performed will not be reversible and hence will not be equal to the free energy. Equation (5.12) can then be identified as the nonequilibrium work  $W$  for this transformation, not the equilibrium free energy  $\Delta G$ . Jarzynski noticed that the free energy of the transformation can be written as the average of the nonequilibrium trajectories that start from an equilibrium ensemble:

$$\Delta G = \beta^{-1} \ln \langle e^{-\beta W} \rangle_0. \quad (5.13)$$

If the switching is instantaneous, then Equation (5.13) becomes identical to EXP because the instantaneous work is simply the change in potential energy. A number of studies have compared nonequilibrium pathways to single-step perturbations. However, in both theory and practice it

appears that under most circumstances, equilibrium simulations are about the same or slightly more efficient than free energies calculated from ensembles of nonequilibrium simulations.<sup>73,86,87</sup> It is thus not clear that free energy calculations using Jarzynski's relationship will have much role in ligand-binding calculations in the future. There has been extensive research in this topic recently, partly because this formalism has proven useful in treating nonequilibrium experiments as well as simulations.

### Bennett acceptance ratio

The free energy computed using EXP in either direction between two intermediate states converges to the same result with sufficient samples. The biases from opposite directions will cancel, which suggests that simple ways to improve EXP are to simply perform the calculation in both directions and average the results or to perform double-wide sampling. However, because of a direct relationship between the distributions of potential energy in the forward and reverse directions,<sup>88</sup> there is a significantly more robust and in fact provably statistically optimal way to use information in both directions. Bennett's original formulation started with a simple relationship for the free energies:

$$\Delta G_{0 \rightarrow 1} = \ln kT \frac{Z_0}{Z_1} = kT \ln \frac{\langle A(\mathbf{x}) \exp[-\beta(H_0 - H_1)] \rangle_1}{\langle A(\mathbf{x}) \exp[-\beta(H_1 - H_0)] \rangle_0}, \quad (5.14)$$

which is true for any function  $A(\mathbf{x})$ . Bennett then used variational calculus to find the choice of  $A(\mathbf{x})$  that minimizes the variance of the free energy,<sup>89</sup> resulting in an implicit function of  $\Delta G$  that is easily solvable numerically. A separate approach demonstrates that the same formula provides the maximum likelihood estimate of the free energy given the observations of the potential energy differences between the two states.<sup>90</sup> Either derivation additionally gives a robust estimate for the variance of free energy. Studies have demonstrated both the theoretical and practical superiority of BAR over EXP in molecular simulations.<sup>73,74</sup> Significantly less overlap between the configurational space of each state is required to converge results than in the case of EXP, although some overlap must still exist.

It is difficult to directly compare TI and BAR on a theoretical basis. However, it appears that TI can be as efficient as BAR under conditions where the integrand is very smooth,<sup>12,73</sup> such as charging or small changes in molecular size, but BAR appears to be significantly more efficient than TI or EXP for free energies of larger molecular changes, sometimes by almost an order of magnitude.<sup>73,74,91</sup> If the intermediate states can be written as functions of the final states, as discussed previously, then the calculations of the potential energy in these alternate states can be very efficient, as only two computations of pairwise interactions are needed. Otherwise, the energies of changing parts of the system must be calculated for each state, which unfortunately is not necessarily implemented in most simulation codes currently.

### WHAM

In most cases, alchemical free-energy computations require simulation at a number of different intermediates, and we would prefer to obtain as much thermodynamic information as possible from all of these simulations simultaneously. If one intermediate is relatively similar to a number of other intermediates, and not just the nearest neighbors, then all of this information can be used to calculate the free energy more precisely. Histogram weighting techniques were first introduced by Ferrenberg and Swendsen<sup>92</sup> to capture all of this information to compute free energies. A version called the weighted histogram analysis method (WHAM) was introduced in 1992 by Kumar and collaborators for alchemical simulations.<sup>93</sup> WHAM is probably the lowest uncertainty method to calculate the free energy for samples collected from discrete states. However, it introduces biases in continuous states (such as those obtained with atomistic simulations) because it requires discretization into bins. Other variations of WHAM based on maximum likelihood<sup>94</sup> and Bayesian methods<sup>95</sup> have also been developed. A version of WHAM-based free-energy calculation is available within the CHARMM molecular mechanics package.<sup>96,97</sup>

### MBAR

It was noted<sup>93,96</sup> that one can reduce the histogrammed equations of WHAM to a simpler form by reducing the width of the histogram to zero, yielding a set of iterative equations to estimate the  $K$  free energies:

$$G_i = -\beta^{-1} \ln \frac{\sum_{k=1}^K \sum_{n=1}^{N_k} \frac{\exp[-\beta H_i(\mathbf{x}_{kn})]}{\sum_{k'=1}^K N_{k'} \exp[\beta G_{k'} - \beta H_{k'}(\mathbf{x}_{kn})]}}, \quad (5.15)$$

where  $i$  runs from 1 to  $K$ , the  $G_i$  are the free energies, and the  $H_i$  are the Hamiltonians of these  $K$  states. This approximation is somewhat suspect, as the derivation of WHAM involves finding the weighting factors that minimize the variance in the occupancy of the bins, which are undefined as the width goes to zero.

A recent multistate extension of the BAR has been derived that solves this problem. In this derivation, a series of  $N \times N$  weighting functions  $A_{ij}(\mathbf{x})$  are adjusted to minimize the free energies of all  $N$  states considered simultaneously. The lowest variance estimator can be seen to exactly be the WHAM equation in the limit of zero-width histograms [Equation (5.15)]. WHAM can therefore be seen as a histogram-based approximation to this multistate Bennett's acceptance ratio (or MBAR).<sup>91</sup> This MBAR derivation additionally gives the uncertainty of the calculated free energies, which is not available in WHAM.

### Choice of alchemical pathways

A key point in these methods is that for almost all alchemical transformations between the initial and final

Hamiltonian, there must be a series of intermediates with mutual phase-space overlap leading connecting the two physical end states. The simplest choice for most transformations between two Hamiltonians  $H_0$  and  $H_1$  is the linear pathway:

$$H(\lambda, \mathbf{x}) = (1 - \lambda)H_0(\mathbf{x}) + \lambda H_1(\mathbf{x}). \quad (5.16)$$

A significant problem with this formulation is that equal spacing in  $\lambda$  does not actually lead to equal spacing in phase-space overlap. If a Lennard–Jones function is used to represent the atomic exclusion and dispersion interaction, as is typically the case in biomolecular force fields, then when  $\lambda = 0.1$ , nearly at the disappearing end state, the excluded volume (i.e., the volume with energy above 2–3  $kT$ ) will still occupy 60–70% of the original volume, depending on the original Lennard–Jones well depth.

Additionally, this choice of parameterization with an  $r^{-12}$  potential leads to a singularity in  $\langle dH/d\lambda \rangle$  at  $r = 0$ , which can be integrated formally but not numerically. By using a power of  $\lambda \geq 4$  instead of a strictly linear parameterization [such as  $H(\lambda) = (1 - \lambda)^4 H_0 + \lambda^4 H_1$ ],  $\langle dH/d\lambda \rangle$  can be numerically integrated correctly. However, it will still converge slowly.<sup>80,99</sup> For any nonzero  $\lambda$ , whatever the power, there will be small “fenceposts,” particles with a small impenetrable core.<sup>99</sup> One possible way to avoid issues with these fenceposts has been to shrink the entire molecular structure. However, this can create problems with nonbonded interactions as the molecular framework shrinks, causing instabilities in integration in molecular dynamics,<sup>99–101</sup> and is generally not practical for large numbers of bonds. A correction term must also be added for these bond length changes, which can be complicated if the bonds lengths are constrained.<sup>102</sup>

There are better ways to handle this transformation. The concept of a “soft core” was introduced around 1994,<sup>82,103</sup> with the infinity at  $r = 0$  in the  $r^{-12}$  interaction being “smoothed out” in a  $\lambda$ -dependent way. The most common parameterizations for turning off the Lennard–Jones function are of the form

$$H(\lambda, r) = 4\epsilon\lambda^n \left\{ \left[ \alpha(1-\lambda)^m + \left(\frac{r}{\sigma}\right)^6 \right]^{-2} + \left[ \alpha(1-\lambda)^m + \left(\frac{r}{\sigma}\right)^6 \right]^{-1} \right\} \quad (5.17)$$

where  $\epsilon$  and  $\sigma$  are the standard Lennard–Jones parameters,  $\alpha$  is a constant (usually 0.5), with the original choice of  $n = 4$  and  $m = 2$ .<sup>82</sup> Further research has shown that using  $n = 1$  and  $m = 1$  noticeably improves the variance.<sup>80,99,104</sup> The more flexible the molecule, the more using a soft atomic core improves the efficiency of the free-energy calculation. Approaches using a soft core for the Coulombic term<sup>82,105</sup> or making all the interactions disappear into an imaginary fourth dimension have also been tried,<sup>106</sup> but it can be difficult to choose parameters for these approaches that are transferable between systems.

Recent studies have demonstrated that one highly reliable, relatively high efficiency pathway for an alchemical

change where an atomic site disappears is to turn off the charges linearly and then turn off the Lennard–Jones terms of the uncharged particles using a soft-core approach. The same pathway can be followed in reverse for atomic sites that are introduced.<sup>97,99</sup> It is the treatment of the singularities at the center of particles that is the real challenge; atomic sites that merely change atom type can be handled with linear interpolation of the potential energy, as the phase-space overlap changes are relatively small with respect to phase-space changes with introduction of particles. The variance due to changes in the bonding terms is not generally a problem; although the energy changes for these terms can be quite large, the time scale of the motions means that they converge quite quickly.

It is likely that further optimizations of pathways may lead to additional efficiency gains. But they will probably not increase efficiency by much more than a factor of 2 as there are limits to the lowest possible variance path.<sup>105</sup> Studies of optimal pathways have focused on minimizing the variance in TI,<sup>82,105</sup> but it appears that highly optimal pathways for TI work well for all other methods.

### Pulling methods

Another choice of pathway for determining the free energy of protein/ligand association is to physically pull the molecule away from the protein. If the final state is sufficiently far from the original protein, the free energy of this process will be the free energy of binding. This can be done either by nonequilibrium simulations, using the Jarzynski relationship, or by computing a PMF using umbrella sampling with different overlapping harmonic oscillators at specified distances from the binding site.<sup>107–110</sup>

There are a number of complications with pulling methods. Pulling a ligand out of a buried site can pose problems, and it can be difficult to pull the ligand sufficiently far away from the protein with a simulation box of computationally tractable size. In the latter case, some analytical or mean-field approximation must be applied for the free energy of pulling the ligand to infinity. However, it has been argued that pulling may be significantly more efficient for highly charged ligands.<sup>108</sup>

### Promising methods not yet routine

Researchers are experimenting with a number of intriguing methods that have significant potential to make ligand-binding calculations much more efficient but that are not yet routine. It is likely that many or all of these will become much more commonplace in the near future. We will give only brief a introduction along with references for further investigation.

### Using umbrella sampling for convergence

A general problem for any free-energy simulation method is sampling important configurations. One standard method

for improving sampling in atomistic simulations is umbrella sampling,<sup>111</sup> where bias terms are added to constrain the simulation in some way and their effect is then removed. This procedure can be used to either lower potential energy barriers or to restrain simulations to slow-interconverting configurations that are relevant to the binding affinity (for example, different torsional states), allowing each of the component energies to be properly computed and then combined.<sup>97,112,113</sup> Another application is computing the free energy of constraining the free ligand into the bound conformation directly before computing the free energy of binding and then releasing these restraints, usually decreasing the correlation times for sampling of the intermediate states and thus increasing the efficiency of the simulation.<sup>97,108</sup>

#### Expanded ensemble, Hamiltonian exchange, and $\lambda$ dynamics

Alchemical simulations usually include a number of intermediate states. It is possible to bring these intermediates together in a single simulation system, either as series of coupled simulations of the intermediate states, usually called Hamilton exchange, or as a single simulation that visits all of the intermediate states, called expanded ensemble simulation. A number of studies have shown that Hamiltonian exchange and expanded ensembles can speed up simulations by allowing the system to go around barriers by going through alchemical states where those barriers are not as pronounced, significantly speeding up free-energy simulations.<sup>114–120</sup> Alternatively, the alchemical variable  $\lambda$  can be treated as a dynamic variable, which adds complications by introducing a fictitious mass corresponding to the  $\lambda$  degree of freedom but is essentially equivalent to Monte Carlo techniques.<sup>118,121–123</sup> There are a number of variations of sampling in  $\lambda$  that may show promise in the future, but such methods are still in the preliminary stages of development.<sup>124–128</sup>

#### Multiple ligands simulations

If binding calculations of multiple ligands with a single protein target can be performed in the same simulation, this can significantly speed up the efficiency of calculations. This has been most successfully done by running a single simulation of a nonphysical reference state and then computing the free energy via EXP to a large number of potential ligands.<sup>97,129,130</sup> However, this frequently fails to work when the ligands are too dissimilar.<sup>131</sup> More sophisticated multi-ligand approaches will most likely be necessary.

### RECENT HISTORY IN LIGAND BINDING CALCULATIONS FOR PHARMACEUTICALLY RELEVANT SYSTEMS

#### MM-PBSA calculations

MM-PBSA has been used in a range of applications for exploring the free energetics of biologically relevant molecules, and reports in the literature appear for a variety

of nontrivial, structure-related problems. Although early applications focused on rationalizing relative conformational stabilities in DNA<sup>132</sup> and RNA,<sup>133</sup> it was not long before attempts to analyze protein/ligand interactions began to appear. For instance, MM-PBSA was used to verify a hypothesis that electrostatic interactions were the primary driver for haptin association with Fab fragments of antibody 48G7.<sup>134</sup> It was also used to elucidate situations in which hydrogen bonding was postulated to be an important contributor to protein/ligand association,<sup>135</sup> to gain insights into the role of hydrophobic interactions in cAMP-dependent protein kinase,<sup>47</sup> and to investigate carbohydrate recognition in concanavalin.<sup>37</sup> Other uses of MM-PBSA include rationalizing the role of  $pK_a$  shifts in protein/ligand binding,<sup>137</sup> and demonstrating the importance of the choice of proper protonation states in the active site.<sup>138</sup> Structure-based ligand design methods have also been built on top of MM-PBSA. One technique, called computational alanine scanning,<sup>139</sup> probes potential interaction sites in receptor binding pockets, and an analogous method was developed for small molecules called fluorine scanning.<sup>140</sup>

The wide range of applications of MM-PBSA reported in the literature reflect its increasing penetration into the scientific community. Based on results from a search of a life sciences citation database maintained by *Entrez*, the number of publications reporting some use of MM-PBSA to perform binding analysis has steadily increased from fourteen total in the two years from 2001 to 2002 to fifty total in the years 2006–2007. The consistent increase in the use of MM-PBSA is likely due to several factors. MM-PBSA has relatively low computational cost compared to other (more rigorous) binding free-energy methods, which broadens the number of systems to which it can be reasonably applied. Several initial reports on MM-PBSA appearing in the literature showed significant potential for the method. In particular, one of the earliest results demonstrated impressive affinity predictions for the protein target avidin binding a set of biotin analogs.<sup>141</sup> Subsequent reports showed equally promising results for affinity predictions for other systems.<sup>142–146</sup>

Because of the early reports a large number of groups have applied MM-PBSA to a wide variety of systems. We can investigate one aspect of the evolution of the use of MM-PBSA by inspecting the literature reports that have appeared over the years from 2001 to 2007. Shown in Figure 5.2 are values (estimated where possible from the publications found in the aforementioned citation search) for the mean-square error (MSE) in reported affinity predictions, as a function of the publication year.

From 2000 to 2003, MM-PBSA reports contained significantly smaller average MSE values in the literature, compared to averages from the span of 2004 to 2007. There are a number of possible explanations for this trend. Early applications may have been restricted to more well-behaved systems appropriate for initial verification and later studies were more representative of the average over many systems.

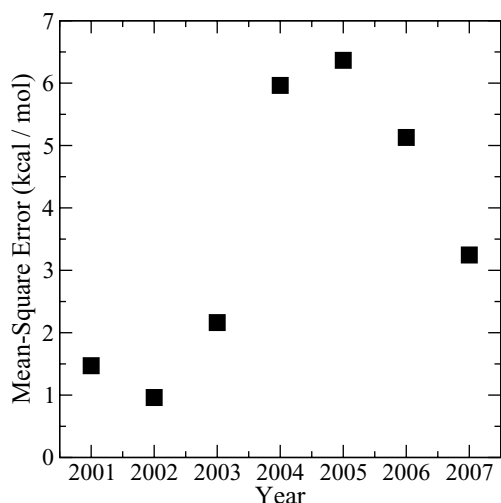


**Figure 5.2.** Errors obtained from literature data showing the progression of estimated mean-square errors for MM-PBSA affinity predictions.

It could also be that MM-PBSA has arrived in the hands of less experienced practitioners, who are less familiar with the subtleties involved. It also may be the case that people are currently more willing to publish less successful applications than has been the case in the past. Whatever the root cause, it seems safe to conclude that (at least for the published reports) there is a different expectation for the potential magnitudes of errors produced by MM-PBSA today than was initially apparent.

To explore the general question of reliability of MM-PBSA, its performance must be examined in a variety of systems. Shown in Figure 5.3 is the change in experimental binding affinity (relative to a known reference compound) plotted versus the percentage change in MM-PBSA “score” (relative to the same reference compound) from an internal Abbott study. The specific procedure used for these calculations has been detailed elsewhere.<sup>146</sup> Briefly, conformational sampling is performed in implicit solvent during which a set of structures are saved and subsequently analyzed for energetics as described under “MM-PBSA.” All solute entropic changes on binding are ignored in these calculations. The MM-PBSA energies are referred to as “scores” to reflect the fact that they are not true free energies. To generate the data in Figure 5.3 MM-PBSA calculations were performed on 480 structures (based on 292 structures obtained from Abbott x-ray crystallography) that spanned eight protein targets, including representatives from a number of families, such as kinases, proteases, peptide signaling proteins, and phosphatases. For the compounds that did not have explicit x-ray crystal structures of the bound small molecule, the binding modes were prepared by selecting a (similar) existing crystal structure and performing a three-dimensional overlay of the small molecule onto the crystallographic binding mode.

The data in Figure 5.3 are partitioned into false positives (FP), false negatives (FN), true positives (TP), and

true negatives (TN). The relatively small number of FN produced in the calculations is worth noting, as FN are highly undesirable in a drug discovery setting, due to the fact that they represent missed opportunities. The presence of FP is less problematic as the threshold for desired MM-PBSA score can be altered to accommodate a desired FP rate. To illustrate this we describe several thresholds for percentage change in MM-PBSA score, yielding differing numbers of FP and TP, as shown in Figure 5.3. It can be seen that to reduce the rate of FP to below 10%, one must accept only those compounds exhibiting positive changes in MM-PBSA score greater than 40%. Given the results obtained with MM-PBSA in this study, it appears that it could be used for virtual library triage to produce enriched lists of ranked compounds. An inspection of the spread of  $\Delta\Delta G_{\text{bind}}$  values at various thresholds reveals that a probable value for an anticipated relative error might be in the 2–3 kcal/mol range, which is comparable to recent errors reported in the literature (see MSE for 2007 in Figure 5.2). Based on analysis presented in the introduction to this chapter, incorporating this level of calculation into the work flow of medicinal chemists might begin to add value to synthetic efforts by reducing the average number of compounds that need to be made.

There have been several recent studies investigating the use of MM-PBSA as a potential routine tool in drug discovery. Kuhn et al. found that small-molecule potency predictions with MM-PBSA are generally unreliable at predicting differences smaller than around 3–4 kcal/mol of relative potency,<sup>147</sup> which is in rough agreement with the conclusions presented above. The authors did find MM-PBSA to be useful as a postdocking filter. In a different study, Pearlman found that MM-PBSA performed extremely poorly, and

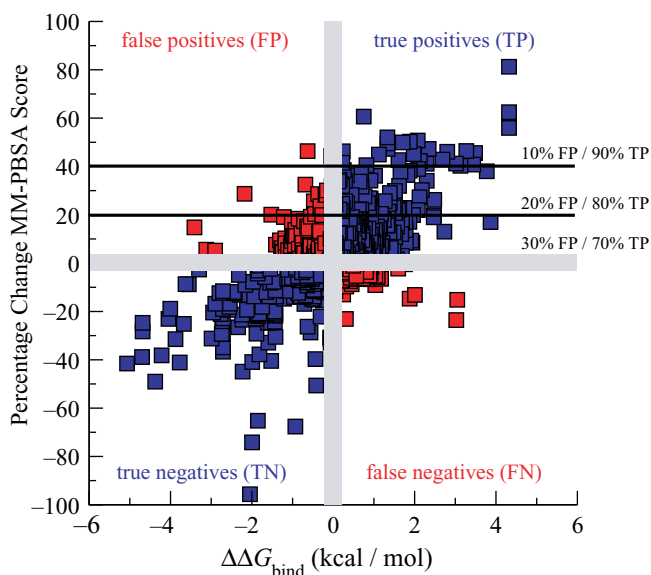


**Figure 5.3.** Data showing change in compound potency (relative to a reference compound) versus percentage change in MM-PBSA score (relative to same reference compound) for 480 compounds across eight targets, which span 292 x-ray crystallographic complexes.

in fact somewhat nonintuitively.<sup>148</sup> This study is somewhat difficult to interpret, as mixed small-molecule force fields were used in addition to normal-mode entropy estimates for all the of data points. In a later publication it was noted that both of the above studies selected molecules with insufficiently wide potency ranges<sup>149</sup>; however, the ranges of potencies in the reports of Pearlman and Kuhn et al. are around 3 kcal/mol, consistent with our findings that MM-PBSA, in general, cannot be expected to reliably resolve compounds within 2–3 kcal/mol. For a sufficiently wide range of potencies careful application of MM-PBSA may provide help and bias discovery effort toward the more potent compounds.<sup>150</sup>

The literature reports other issues with MM-PBSA, for example, in systems including in the presence of a metal ion in the binding site.<sup>151</sup> Inadequacies of MM-PBSA to accurately represent first-solvation-shell effects were shown to introduce significant error into direct potency prediction.<sup>170</sup> However, despite the first-solvation-layer error, MM-PBSA was still able to successfully rank-order the ligands.

There appears to be an emerging consensus that MM-PBSA likely has some applicability and utility in drug discovery. However, results have ranged too widely, from promising to poor to difficult, to interpret unambiguously. There is as of yet insufficient data to conclusively demonstrate the scope, the limitations of MM-PBSA, and the fundamental reliability in industrial drug discovery research, though the studies described here demonstrate enough promise to focus more effort on these methods in the future.

### Alchemical calculations

Alchemical free energies are substantially more rigorous than MM-PBSA calculations but also significantly more computationally demanding. They were first applied to protein/ligand systems in the early to mid-1980s. Tembe and McCammon<sup>152</sup> laid out some of the basic theory for applying these calculations to protein/ligand interactions and used them to examine the “binding” of two Lennard–Jones spheres in a small bath of Lennard–Jones spheres in 1984. This was probably the first “alchemical” free-energy calculation, although the term itself originated somewhat later. The first applications to true protein/ligand complexes followed shortly, with Wong and McCammon computing relative binding free energies of three trypsin inhibitors<sup>153</sup> with some success, and Hermans and Subramaniam computing the binding free energy of xenon to myoglobin.<sup>154</sup> This and related work from others ushered in a wave of alchemical applications in the late 1980s and early 1990s.

However, in a recent review, David Pearlman noted that some of the early success with alchemical methods may have been simply luck. He argues, “[W]e are now at a point that is, in reality, where we thought we were 20 years ago!”<sup>155</sup> At the very least, performing accurate alchemical free-energy calculations has turned out to be a great deal more difficult and computationally demanding than originally

thought,<sup>8,156</sup> so enthusiasm waned after the initial success before undergoing a resurgence since the early 2000s. This recent change has been described as a “coming of age.”<sup>165</sup> Alchemical methods have yet to see widespread use in pharmaceutical applications, however.

Part of the recent increase in enthusiasm for free-energy calculations has been due to some of the methodological innovations addressed above, including the movement away from EXP, and another large part has been due to steadily increasing computer power bringing new problems into range. Together, these factors mean that much of the work on alchemical methods before the early 2000s is woefully out of date, so in this discussion we focus mostly on work since 2000. As noted above, alchemical free energies can be calculated by TI, EXP (exponential averaging), or BAR, among other methods, but the basic ideas remain the same. Here we highlight some key applications areas of alchemical methods without focusing on methodological issues highlighted above.

### Relative free energies

Relative binding free energies were one of the earliest applications of alchemical methods, and they have remained a traditional application of alchemical free-energy methods. Relative free-energy calculations involve alchemically transforming one ligand into another, allowing direct calculation of the relative binding free energies from an appropriate thermodynamic cycle. This may be substantially more efficient than computing two absolute binding free energies and subtracting in cases where the ligands are relatively similar, as it eliminates statistical noise due to transformation of the rest of the ligands. If the limiting factor in the precision of the calculations is a long time-scale conformational fluctuation of the protein, however, the relative efficiency of relative free-energy calculations may be lessened considerably.

There have been a number of practical success stories with these calculations. One particularly interesting and comprehensive set of studies has been work from the Jorgensen lab on binding of HIV-1 nonnucleoside reverse transcriptase inhibitors (NNRTIs).<sup>157–163</sup> One study used docking and molecular dynamics equilibration to generate a model structure of sustiva bound to HIV-1 reverse transcriptase and then alchemical free-energy methods with Monte Carlo conformational sampling to compute the change in binding affinity of sustiva due to several known drug resistance mutants. Because the computed drug resistance profile matched well with experiment (with relative binding free energies accurate to 1–2 kcal/mol), this suggested that the model binding mode was indeed correct, a fact that was subsequently confirmed crystallographically.<sup>157</sup> Two other studies examined effects of known drug resistance mutations on several inhibitors and derivatives<sup>158,159</sup>; both were accurate to within 1 kcal/mol in relative binding free energies. One issue with these calculations concerns the approximations made, including the

fact that the protein backbone was fixed and only side chain atoms within 15Å of the ligand were allowed to move, which is worrisome given the fact that HIV-1 NNRTIs allosterically disrupt enzymatic activity at a site that neighbors the binding pocket. Three other studies describe the application of free-energy calculations to lead optimization and the resulting compounds' activity in a cell-based assay; no affinity measurements were made, so no quantitative assessment of accuracy is possible.<sup>160,161,163</sup>

In several other cases, relative free-energy calculations have been used to validate models and suggest mechanisms. As noted above, relative free-energy calculations were used to validate the modeled binding mode of sustiva in HIV-1 reverse transcriptase. Relative free-energy calculations were also used to validate a homology model of a G-protein-coupled receptor by computing relative binding affinities of several known inhibitors<sup>164</sup> with errors of less than 1 kcal/mol. This approach was suggested to be a general one for validating homology models.<sup>156-164</sup> On the mechanism side, Yang et al. used relative free-energy calculations to help identify the tight binding site for ATP in F1-ATPase,<sup>165</sup> and Banerjee et al. used relative free-energy calculations to elucidate the recognition mechanism of oxo-guanine by a DNA repair enzyme.<sup>166</sup>

There has also been a significant amount of work with relative free-energy calculations on the estrogen receptor, mostly using artificial intermediate states designed to allow rapid estimation of free energies of multiple different inhibitors from just one or two simulations.<sup>87,129,167</sup> The downside is that phase-space overlap issues due to the limited number of simulations can present convergence problems, so the quality of the results has been very mixed depending on the choice of reference state, with errors ranging from nearly 0 kcal/mol up to more than 20 kcal/mol.<sup>87</sup>

Another system of interest is fructose 1,6-bisphosphatase, where alchemical free-energy calculations have been used over many years to help guide lead optimization with some degree of success. A recent discussion is provided by Reddy and Erion.<sup>168</sup> Though extremely short simulations were used, with some other methodological limitations, alchemical calculations appear to have helped the lead optimization process.

Alchemical calculations have also been applied successfully to inhibitors of neutrophil elastase. A multistep procedure involving docking, then MM-PBSA scoring to identify binding modes, followed by thermodynamic integration to calculate relative binding free energies, gave results for relative binding free energies within 1 kcal/mol.<sup>169</sup> In a follow-up study, alchemical calculations were used to predict a modification to an inhibitor to increase the affinity. When synthesized, the new inhibitor had an IC<sub>50</sub> value that was a factor of 3 better.<sup>213</sup>

Alchemical calculations have given good correlations with experimental relative free energies for relative binding free energies of theophylline and analogs to an RNA

aptamer.<sup>170,171</sup> One recent study also examined two trypsin inhibitors with a polarizable force field,<sup>172</sup> and another study with a polarizable force field examined a series of inhibitors of trypsin, thrombin, and urokinase and observed an excellent correlation with experimental relative binding affinities.<sup>173</sup> A series of relative free-energy studies have also examined binding of peptide and nonpeptide inhibitors of Src SH2 domains with mixed results.<sup>174-177</sup>

Several other studies have focused on the practical utility of free-energy calculations. Pearlman and Charifson compared alchemical free-energy calculations with more approximate methods on a challenging system and suggested that they have reached the point where they can be useful, and more predictive than other methods, in drug discovery applications; the test examined p38 MAP kinase.<sup>178</sup> A follow-up study showed that alchemical methods compared favorably with MM-PBSA in terms of accuracy and computational efficiency.<sup>148</sup> Another study by Chipot argues that the accuracy of alchemical methods is now sufficient to be useful in drug discovery, and the main remaining hurdle for their widespread application is how difficult they are to set up.<sup>156</sup> A further study by Chipot and coauthors shows that these calculations can be in some cases done quite rapidly and still yield accurate rank-ordering,<sup>176</sup> further highlighting the potential utility of alchemical methods. Another particularly interesting application was the computation of implicit solvent alchemical free energies of several different protein/ligand systems, where free-energy methods compare very favorably with docking, with much greater speed than with explicit solvent methods.<sup>229</sup>

### Absolute free energies

Alchemical binding free-energy calculations have mostly been restricted to computing relative binding free energies. Computing the absolute binding free energy of a single ligand to a particular protein introduces two additional complexities not ordinarily encountered in relative free-energy calculations. An early (1986) article on protein/ligand binding highlighted both of these issues.<sup>154</sup> First, absolute binding free energies are reported relative to a standard state or reference concentration of ligand, so a reference concentration must somehow be introduced into the relevant thermodynamic cycle. Second, if a ligand does not interact with the rest of the system (as in an alchemical absolute binding free-energy calculation) it will need to sample the whole simulation box for convergence, presenting potential sampling problems that are discussed in more detail elsewhere.<sup>153</sup> The authors' solution to these problems was to introduce biasing restraints that both kept the ligand in the binding site when noninteracting and simultaneously introduced the standard state when the effect of the restraints is analytically accounted for. The clearest and most detailed discussion of these issues is provided by the excellent review of Gilson,<sup>180</sup> which laid the foundation for recent applications of binding free-energy calculations. A

recent review of absolute free-energy calculations is provided by Deng and Roux.<sup>181</sup>

Despite the fact that these issues were raised in the 1986 work, a variety of “absolute” binding free-energy calculations since then have neglected one or both of these issues. Nevertheless, beginning in the mid-1990s, there have been a number of successful applications of absolute binding free-energy calculations. These cluster in three general categories that each merit individual discussion: (1) binding of water within buried sites or binding sites of proteins, (2) binding of nonpolar ligands in a designed binding cavity within T4 lysozyme, and (3) binding of ligands to FKBP.

**Water binding.** The area of water binding is particularly interesting (and challenging) because it is extremely difficult to access the thermodynamics of water binding experimentally, meaning that computation uniquely provides access to important and interesting information. It represents an important application of free-energy calculations that does not simply serve to predict a binding affinity but also adds physical insights about the binding process that can also be used in the further design. One important computational challenge is to ensure that the water molecule being removed is not replaced by any other water molecules while being removed, or else the net result of the calculation will simply be to remove a water molecule from bulk. This methodological issue is not always addressed in work on water binding and in some cases may be a concern.

Work in the area of water binding was begun with the absolute binding free-energy calculations of Helms and Wade in 1995. They found that a crystallographic water bound in a cavity in cytochrome P450cam with a particular inhibitor had a binding free energy around  $-2.8 \pm 1.6$  kcal/mol while transferring a water into the cavity with the natural substrate (camphor) would cost  $3.8 \pm 1.2$  kcal/mol. A follow-up study found the preferred number of water molecules in the cavity in the absence of ligand,<sup>182</sup> finding that six waters is thermodynamically preferable over five and seven or eight by 1–2 kcal/mol. A third study then computed the absolute binding free energy of camphor by replacing it with six waters in the binding site.<sup>183</sup> More recently, Deng and Roux applied alchemical free-energy calculations in combination with a grand canonical Monte Carlo scheme to replace camphor with water molecules while removing camphor from the cavity.<sup>184</sup> Their computed binding free energy for camphor agreed fairly well with that of Helms and Wade, but they differed slightly on the number of water molecules in the cavity.

Another water binding free-energy study examined the binding of crystallographic waters in the subtilisin Carlsberg complex with eglin-C and found that only some of the waters appeared to bind favorably.<sup>185</sup> Another study (on bovine pancreatic trypsin inhibitor and a barnase mutant) reached similar conclusions about crystallographic waters,<sup>186</sup> and a more recent study has also observed unfavorable binding energies for crystallographic waters.<sup>187</sup>

The reasons for this apparent discrepancy are so far unclear, but one suggestion has been limitations in the force field,<sup>186,187</sup> partly because the crystallographic waters are often conserved across several different structures of the same complex or binding site, suggesting that crystal structure uncertainties may not be the problem.

Several studies have examined binding of a specific water (water 301) in the complex of HIV-1 protease with inhibitor KNI-272. Two studies agreed on the binding free energy of this water (around  $-3.3$  kcal/mol for one protonation state of the protease),<sup>188,189</sup> while a third study disagreed by about 7 kcal/mol,<sup>187</sup> possibly due to methodological differences relating to the treatment of protein flexibility. The active site protonation state appears to substantially modulate the binding free energy of this water molecule.<sup>189</sup>

There have been a variety of other examinations of water energetics as well. Roux et al. looked at binding of several waters within bacteriorhodopsin and found that transfer of waters from bulk to the proton channel was thermodynamically favorable (in some cases by up to 6 kcal/mol), suggesting implications for proton transfer.<sup>190</sup> De Simone et al. looked at water binding within the prion protein.<sup>191</sup> An extensive study looked at binding free energies of fifty-four water molecules in binding sites of six proteins, with and without ligands present. As validation, some results were compared with previously published work before moving to new binding sites. Overall, water binding free energies varied substantially, with a mean binding free energy of  $-6.7$  kcal/mol, substantially more favorable than the mean binding free energy of water molecules that are displaced by ligands ( $-3.7$  kcal/mol). The range of binding free energies runs from slightly positive to around  $-10$  kcal/mol.<sup>187</sup> One major conclusion from this and the other studies in this area is that water molecules make a highly variable contribution to the thermodynamics of ligand binding, and factoring water molecules into ligand design is likely not to be an intuitive process, thus increasing the need for computational methods that can account for variable contributions of bound waters.

A final study worthy of note for its novelty and potential practicality for drug discovery is the work of Pan et al., which used a grand canonical Monte Carlo technique to qualitatively predict locations around binding sites where waters can easily be displaced, suggesting routes for lead optimization.<sup>192</sup> Although this is not an application of absolute alchemical free-energy methods, it is nevertheless an extremely interesting application of free-energy methods to water binding.

**T4 lysozyme ligand binding.** Another important set of systems for studying binding free-energy calculations are the two model binding sites in T4 lysozyme created by point mutations. The first of these, the L99A mutant, introduces a simple nonpolar cavity, while the second (L99A/M102Q) adds a polar group at the margin of the cavity and introduces the possibility of more hydrogen bonding. Both have been extensively characterized

experimentally.<sup>113,193–199</sup> Because these binding sites are relatively simple and rigid, and structural data are so easy to obtain, they have been attractive sites for the development and testing of absolute free-energy methods. Most of the work has been on the apolar version of this cavity.

One early absolute free-energy study, in 1997, examined the binding of benzene in the apolar cavity.<sup>200</sup> Depending on the computational details, calculated values range from  $-4.0$  to  $-5.1$  kcal/mol, and the experimental absolute binding free energy is  $-5.2$  kcal/mol. A follow-up study examined binding of noble gases in the cavity, especially xenon, which binds under pressure, in agreement with computed binding free energies.<sup>201</sup>

The lysozyme cavity was also used as a test system for the methodological work of Boresch et al. in 2003, which fell short of actually computing a binding free energy, but laid out a clear and straightforward thermodynamic cycle for computing binding free energies; the cycle involves the use of both orientational restraints and distance restraints.<sup>202</sup> Work on the polar cavity extended some of the arguments in favor of using orientational restraints and found that large kinetic barriers can separate ligand orientations, so considering multiple candidate bound orientations can help when computing absolute binding free energies.<sup>179</sup>

More recent work done by Deng and Roux<sup>203</sup> looked at a series of known binders to the lysozyme cavity, with somewhat mixed success; some binding free energies were too negative by a few kcal/mol. Another study used grand canonical Monte Carlo techniques on the same system, but while neglecting protein flexibility,<sup>204</sup> again with mixed success. A third looked at binding of a single ligand in the lysozyme cavity and quantified the contributions of a slow side-chain motion to ligand binding. It found that a single side-chain rearrangement could affect binding free energies by a few kcal/mol and that including the free energies associated with this conformational change was key for obtaining accurate binding free energies.<sup>205</sup>

The most extensive study to date has been the joint theory-experiment work of Mobley, Graves, and others,<sup>113</sup> which studied a variety of previously measured ligands and reached a root-mean-square error of roughly 1.9 kcal/mol after dealing with problems relating slow sampling of ligand orientational changes, protein conformational changes, and ligand electrostatics parameters. A unique feature of this study was that bound crystal structures were not used as starting points for the calculations, except for comparison purposes. Absolute free-energy methods were then applied successfully to predict binding affinities, with errors less than 0.7 kcal/mol, and orientations of five previously untested small molecules. The contribution of protein flexibility was also assessed and turned out to be key for the accuracy of the results.

Overall, a message from the lysozyme work has been that even simple binding sites can present significant sampling problems for molecular simulations, especially concerning ligand orientations and side-chain degrees of freedom and

that a proper accounting of the thermodynamics here is key for obtaining predictive results.

**FKBP binding calculations.** The FK506 binding protein (FKBP) has been another popular test system for absolute free-energy methods, in part because of the relative rigidity of its backbone. FKBP-12 was important in the development of the immunosuppressive drug cyclosporin and has remained popular because of its role in the development of the field of chemical biology. A series of ligands studied experimentally by Holt et al. have been studied particularly closely by a number of researchers.<sup>206</sup>

Absolute alchemical free-energy methods were first applied to the system by Shirts,<sup>207</sup> who obtained root-mean-square error of 2.0 kcal/mol and a correlation coefficient ( $R^2$ ) of 0.75. A follow-up study by Fujitani and collaborators<sup>208</sup> achieved a root-mean-square difference from a linear fit of only 0.4 kcal/mol, but with a large offset of  $-3.2$  kcal/mol relative to experiment. As previously noted,<sup>10</sup> care must be taken when comparing this study directly with other absolute free-energy studies, because it neglects any treatment of the standard state, which could be part of the reason for the offset.<sup>179</sup>

A further study by Wang, Deng, and Roux using the same parameters as Shirts obtained a root-mean-square error around 2.0–2.5 kcal/mol,<sup>97</sup> but despite the fact that the results used the same parameters, they were significantly different from those of Shirts,<sup>207</sup> suggesting methodological or convergence differences. Another study by Jayachandran and coworkers obtained a root-mean-square error of 1.6 kcal/mol using a novel parallelized free-energy scheme that allows for contributions of multiple kinetically distinct ligand orientations.<sup>209</sup>

Two other smaller studies also applied absolute free-energy methods to the same system, although not alchemical free-energy methods. The work of Lee and Olson used PMF techniques to compute binding free energies of two inhibitors<sup>106</sup> with accuracies of 1–2 kcal/mol depending on the solvent model, and Ytreberg used nonequilibrium pulling techniques for two inhibitors with accuracies around 1 kcal/mol.<sup>109</sup>

In many cases, computed values have varied substantially, even when using the same parameters. Likely, full convergence has not yet been truly reached. This provides a warning for computations on the many systems that have significantly more conformational flexibility and an indication that higher accuracy with systems that have not been studied as systematically might result from some degree of coincidence.

**Other interesting binding calculations.** Absolute free-energy methods have also been applied in several other interesting cases where there is less of a body of work. Recently, Jiao et al. calculated the absolute binding free energy of benzamidine binding to trypsin using AMOEBA, a polarizable force field, and then computed the relative binding free energy of a benzamidine derivative<sup>172</sup> with accuracies to within than 0.5 kcal/mol. Due to the small size

of the study, it is difficult to be sure whether the high accuracy here is fortuitous or because of the use of a polarizable force field itself.

Dixit and Chipot also applied absolute free-energy calculations to compute the binding free energy of biotin to streptavidin; they obtained  $-16.6 \pm 1.9$  kcal/mol compared to an experimental value of  $-18.3$  kcal/mol.<sup>210</sup>

### Solvation free energies

Alchemical free-energy methods have often been tested by or applied to computing hydration free energies of small molecules like amino acid side-chain analogs or other small neutral compounds,<sup>81,205,211</sup> occasionally in a predictive context.<sup>212</sup> These tests can provide insight into the fundamental level of accuracy that can be expected of current force fields and also provide guidance for improvements to force fields. Also, several studies have highlighted the fact that solvation of small molecules can play an important role in determining binding free energies. One recent study found that the affinity of two trypsin inhibitors for water was very different, but these differences nearly canceled with differences in the binding site.<sup>172</sup> Another study suggested that solvation free energies played a substantial role in determining the change in binding affinity when optimizing fructose 1,6-bisphosphatase inhibitors.<sup>168</sup>

### Predictive tests

Predictive tests of alchemical free-energy methods have been relatively rare, but at the same time are especially valuable for two reasons. First, to apply these methods in the context of drug discovery, they need to be predictive, and so testing them in a predictive context is a more realistic. Second, when doing retrospective studies, it is easy to be unintentionally influenced by the existing experimental results. For example, one might perform several sets of binding free-energy calculations with altered parameters and conclude that the “correct” set is the set that agrees best with experiment. Was any variation with parameters due to (a) the parameters themselves or (b) random errors due to poor convergence? And how would one proceed in a predictive setting?

However, alchemical free-energy methods have been applied predictively (together with or in advance of experiment) in a few studies. Here we focus especially on cases where experimental results are known and pass over those where we are not aware of any experiment that tests the computational results.

A number of studies have applied alchemical methods in the context of lead optimization. Some of the work from the Jorgensen lab on HIV-1 NNRTI has been predictive,<sup>157,160,161</sup> where free-energy calculations were used to help identify a binding mode and guide lead optimization. Similarly, the work on fructose 1,6-bisphosphatase has been predictive and applied in drug discovery.<sup>168</sup> Alchemical methods have been used to

successfully predict an optimization of a neutrophil elastase inhibitor that was subsequently synthesized and tested.<sup>213</sup> Another application in lead optimization used grand canonical Monte Carlo techniques to guide lead optimization.<sup>192</sup>

Alchemical free-energy calculations were also used predictively, or at least in a joint theory-experimental study, in examining binding of benzamidium derivatives and their binding to trypsin.<sup>214</sup> The computational results correctly captured experimental trends, though falling short of quantitative accuracy. A joint theory-experiment study that examined relative binding free energies of inhibitors to a GPCR was used to help validate a homology model; the computational results proved accurate to less than 1 kcal/mol.<sup>164</sup> Alchemical free-energy calculations were also used to predict the tight binding site of ATP in F1-ATPase,<sup>165</sup> a prediction subsequently confirmed experimentally.<sup>215</sup>

The only predictive absolute binding free-energy calculation we are aware of to date is the work on the T4 lysozyme system by Mobley, Graves, and collaborators, where absolute free energies were used to predict binding affinities and binding modes of several new ligands.<sup>113</sup>

### Pitfalls and negative results

Negative results and failures can in some cases be extremely informative, especially when it is possible to identify failures with specific issues, because in such cases the failures highlight the importance of certain factors. Unfortunately, negative results and failures are not always published, so it can be difficult to gather information in this area, and it is often even more difficult to trace failures back to specific issues. Nevertheless, there are several articles that highlight issues in this area – either by tracing failure to a specific cause or by identifying and avoiding a potential pitfall.

One major, common pitfall is a dependence of computed free energies on starting structure. Because a binding free energy is a ratio of partition functions, it involves integrals over all of the relevant configurations of several systems and thus must be independent of the starting configurations of the system. Unfortunately, computed results often depend on the starting configuration of the system – for example, different starting ligand orientations or different starting protein structures may give different results, as noted in a number of studies. This kinetic trapping is inevitable whenever energy barriers are sufficiently large.<sup>217</sup> Mobley et al. found that results could depend significantly (by more than 1 kcal/mol, in some cases) on starting ligand orientation.<sup>179</sup> In FKBP, Shirts<sup>206</sup> and Wang et al.<sup>97</sup> found that computed binding free energies could differ by more than 1 kcal/mol depending on the choice of starting protein/ligand configuration, and Fujitani et al. also observed a dependence on starting structure.<sup>208</sup> An even larger dependence on the starting protein conformation was observed in lysozyme, where computed values could

differ by 3–5 kcal/mol depending on the starting configuration of a valine side chain.<sup>112,113,203</sup> In another study of HIV-1 NNRTIs, computed relative binding free energies had the wrong sign (an error of roughly 4 kcal/mol) when beginning from a crystal structure with an alternate rotamer conformation near the active site.<sup>63</sup> As noted previously, these are not simply issues of having a wrong protein structure: when protein conformational changes occur on binding, multiple metastable configurations are relevant.<sup>112</sup> Thus, some authors have suggested starting simulations from different regions of phase space as a test for these sorts of issues<sup>111,155</sup> or have in some cases performed this test.<sup>112,155</sup>

Another potential pitfall is the possibility of multiple potentially relevant bound ligand orientations that can be separated by kinetic barriers.<sup>179</sup> This has been observed not only in absolute free-energy calculations on the lysozyme binding site, where interpretation and analysis is simplest,<sup>113,179</sup> but also in relative free-energy calculations for ligands binding to neutrophil elastase<sup>169</sup> and the estrogen receptor.<sup>129</sup> Ligand symmetries can also play a complicating role.<sup>167,179</sup>

In many cases, failures are more difficult to interpret. In a recent study on squalene-hopene cyclase inhibitors, relative free energies computed with a single-step perturbation method had large errors and in some cases had the wrong sign;<sup>131</sup> this was also the case in a study by some of the same authors on phosphodiesterase inhibitors.<sup>216</sup> Another study with single-step methods found results of varied quality depending on the (in principle arbitrary) choice of reference state, indicating poor convergence,<sup>87</sup> and in some cases resulting in very large errors. These errors may mostly be due to poor phase-space overlap with the single-step approach.

Using multiple routes around the same thermodynamic cycle can be a helpful way to check for errors when doing relative free-energy calculations. This approach was used by de Graaf et al.<sup>218</sup> and found very different results depending on the choice of pathway (indicating convergence problems along at least some pathways); cycle closure errors were up to 4.9 kcal/mol and for some paths and mutations, the sign of the relative free energies was even incorrect. Cycle closure errors were also large in the work of van den Bosch et al.<sup>219</sup> Of course, cycle closures only provide a lower bound on the error, and in some cases true errors are much larger than the cycle closure error, as is the case with the large cycle closure error and even larger true error in the work of Dolenc et al.<sup>220</sup>

In many cases, studies may have simply been somewhat too ambitious. Donnini and Juffer attempted to use absolute free-energy calculations to examine binding free energies between peptides and proteins and concluded that “it generally proved rather difficult to predict the absolute free energies correctly, for some protein families the experimental rank order was reproduced. . . .”<sup>221</sup>

### Other types of binding free-energy studies

There are several other types of rigorous binding free-energy calculations that have occasionally been applied to interesting biomolecular problems. Grand canonical Monte Carlo (GCMC) techniques have been used in several applications to compute insertion free energies; in one study these techniques were used to compute favorable sites for displacing waters around a ligand in a binding site,<sup>192</sup> and in another case GCMC techniques were used to estimate binding free energies of ligands to the lysozyme model binding site, though in the absence of protein flexibility.<sup>204</sup> More recently, grand canonical techniques were used to insert water molecules into a protein/ligand binding site while the ligand was being alchemically removed, thereby speeding convergence.<sup>184</sup> Potential of mean force (PMF) methods have also been applied to several protein/ligand systems, including the binding affinities of FKBP inhibitors<sup>107</sup> and the binding affinity of a phosphotyrosine peptide to the SH2 domain of Lck.<sup>108</sup> Nonequilibrium free-energy methods have also been applied to FKBP inhibitors and peptides binding to the SH3 domain.<sup>109,110</sup>

As mentioned previously, the mining minima approach of Gilson and collaborators is also particularly interesting and has given promising results in calculations of binding free energies for host/guest systems<sup>66</sup> and ligands to artificial receptors.<sup>164</sup> However, because of computational limitations, it is difficult to apply it to the protein/ligand systems that are of interest in drug discovery. One recent study used this approach, however, to assess changes in HIV protease inhibitor configurational entropy on binding.<sup>68</sup>

### DIRECTIONS FOR LIKELY IMPROVEMENT

There are a number of different aspects in which free-energy calculations will need to improve to become more accurate and reliable. One of the most important is in the realistic treatment of the environment of the protein/ligand systems. Typical ligand binding simulations include only the protein, the ligand, water, and perhaps a few ions to neutralize the simulated system. But many ligand binding affinities have significant dependence on pH, salt concentration, and metal-ion concentration. None of these additional aspects are typically modeled in ligand binding free-energy calculations and will need to be treated better in the future.

It is also likely that there will need to be further advances in atomistic force field parameters. A number of tests of solvation free energies have demonstrated that the current generation of force fields have fundamental problems that may restrict the ability of these force fields to obtain binding free energies that are accurate to within 1 kcal/mol.<sup>81,104,205,222</sup> Most common force field protein parameters are more than ten to fifteen years old, and only the torsions have generally been improved.<sup>223,224</sup> The

criteria used for validity of protein parameters is usually proper structural conformational preferences, which may not be sufficiently accurate for their use in protein/ligand binding calculations. A recent version of the GROMOS force field, 53A6 has parameters that were fit to free-energy calculations of the free energies of transfer between water and cyclohexane, a first for an atomistic force field.<sup>232</sup> It seems likely that parameterizing to phase transfer properties should result in higher accuracy for binding affinity calculations, which are essentially transfers to a heterogeneous liquid phase, though direct comparisons between force fields optimized to pure liquid properties and transfer free energies have yet to be made.

Even more problematic are sufficiently accurate ligand parameters, as the number of functional groups is significantly higher than for protein systems and the amount of time that has been invested for parameterization significantly lower. Typical ligand parameters might be taken from the generalized Amber force field (GAFF),<sup>225</sup> usually using the ANTECHAMBER program in the AMBER distribution for atomtyping, although it is also sometimes done by hand, and the AM1-BCC method<sup>226,227</sup> (implemented in a variety of software codes) to determine the charges. Schrödinger also has automatic tools to assign atom types of novel compounds within the OPLS-AA parameterization system. Relatively few force fields have associated tools or even algorithms for determining compatible (let alone validated) ligand parameters.<sup>228</sup>

A number of research groups are actively developing polarizable potential functions,<sup>228</sup> which have the potential to greatly improve macromolecular force fields' abilities to predict binding affinities by adding an extra level of physical detail. However, at this point, it is not clear that any of them yet are quantitatively better than fixed charge force fields, as few of them have been validated to the extent that fixed charge models have. Polarizable molecular models are significantly slower than fixed charge models, and therefore both the iterative improvement of such force fields and the development of tools useful for production runs for free-energy calculations will be substantially behind that of fixed charge force fields.

## CONCLUSIONS

As we have seen in this chapter, free-energy calculations are not at the present time generally reliable methods to predict binding affinity and are not currently truly a part of standard structure-based drug design methods. And they certainly are not, and will not anytime in the near future, "black-box" methods that will "automagically" allow determination of free energies without significant investment in the physical chemistry and biology of the system. Although many papers are being published computing binding free energies in retrospective case studies, there is still a lack of comparative studies presenting results over large numbers of systems, with even fewer purely predictive studies. Partly

for these reasons, quantitative free-energy calculations are not a vital part of the discovery work flow of most major pharmaceutical company as far as we aware.

However, such calculations are certainly much closer to usability than they have been in the past. In particular, several recent studies mentioned in this chapter have highlighted the advantages of alchemical relative free-energy calculations compared to approximate methods like MM-GBSA and docking.<sup>130,178,229</sup> Alchemical methods have also been successfully applied in a lead-optimization context<sup>161,230</sup> (and see references therein). It appears that in this area free-energy calculations are already becoming useful but with large remaining hurdles to their more widespread adoption. Such hurdles include not only the computer time needed but also the human time and biochemical knowledge required to set up these simulations.<sup>156,176,218,229</sup>

As we have presented in this chapter, the methods used for free-energy calculations are changing rapidly. Major molecular simulation codes, such as AMBER, CHARMM, NAMD, GROMACS, and GROMOS, are undergoing major improvements and changes in the features used to compute binding free energies. Although these changes will likely greatly improve the ability to perform free-energy calculations, ongoing changes make it difficult to put together stable work flows for preparing ligands and simulation structures and determining ideal free-energy protocols without significant human effort, and it is difficult to recommend particular codes for the easiest use at the present time. MCPRO, developed in the Jorgensen lab, which has recently begun to be distributed by Schrödinger as MCPRO+, although not including much of the most recent methodology (such as Bennett Acceptance Ratio methods or soft-core alchemical pathways), is likely the easiest to use and set up and was used successfully for the HIV-1 NNRTI work in the Jorgensen lab described in this chapter.

One ongoing problem has been the lack of extensive experimental high-accuracy ligand binding affinities. As we have discussed, a desirable goal for free-energy calculations is to reach an accuracy threshold of 1 kcal/mol. However, the majority of experimental measurements, unless using highly accurate methods like ITC or SPR or extremely well-tuned competitive binding affinity assays, many not be more accurate than this, making large-scale validation of computational methodologies difficult. A number of academic databases of protein/ligand structures and interactions have been created, such as <http://www.bindingmoad.org/> and <http://lpdb.chem.lsa.umich.edu/> at the University of Michigan, <http://www.bindingdb.org> at Johns Hopkins, <http://www.agklebe.de/affinity> at Phillips-Universität Marburg,<sup>230</sup> and <http://www.pdbcal.org> at Indiana, but the degree of validation and utility of these databases are not well established.

In the United States, a recently announced NIH NIGMS RFA to establish a national Drug Docking and Screening Data Resource represents an attempt to increase the public availability of high-quality experimental data sets required

for developing, validating, and benchmarking computational screening, docking, and binding affinity prediction, including both curating crystal structures and experimental binding affinities (see NIH NIGMS RFA-GM-08-008). NIST has recently become interested in developing and curating such data as well. Most importantly, there is a much larger wealth of data in proprietary pharmaceutical databases that no longer has significant intellectual property value, and a system for releasing such data to the broader community would be immensely valuable for development of improved drug design methods.

Another problem in the development of free-energy techniques is that most large-scale validations and comparisons of methodologies have been retrospective. There are relatively few opportunities to participate in large-scale prospective trials, as confidence of experimentalists in quantitative predictions made by computer is usually not high enough to motivate the high-quality experiments that can validate the computational results.

The quality of techniques for protein structure prediction has increased since the introduction of CASP (Critical Assessment of Structure Prediction) in 1994. Despite some criticisms about some aspects of the program,<sup>232</sup> it is considered to have played an important role in developing computational structure prediction. Other successful ongoing prospective computational challenges have been CAPRI (Critical Assessment of PRedicted Interactions) for protein/protein complexes,<sup>233</sup> the Industrial Fluid Properties Simulation Collective (IFPSC) (at <http://www.fluidproperties.org>), the Cambridge Crystallographic Data Centre's blind tests of small-molecule crystal structure prediction,<sup>234</sup> and the McMasters high-throughput screening competition.<sup>235</sup> It is clear that providing an opportunity for truly blind predictions of chemical and biological properties structure has been beneficial for the computational methodology community. There has therefore naturally been an interest in developing a similar true prospective trial for prediction of ligand binding affinities.

One such attempt called CATFEE (Critical Assessment of Techniques for Free Energy Evaluation) was attempted in 2000 but failed because the experimental data never became available.<sup>236</sup> A more recent attempt, called SAMPL (Statistical Assessment of the Modeling of Proteins and Ligands), run by OpenEye Software, was conducted in late 2007 to early 2008, with two protein targets (urokinase, with data contributed by Abbott, and JNK3 kinase, with data contributed by Vertex) and sixty-three ligand binding points determined by IC<sub>50</sub>s, but with the same assay for each target. The competition consisted of virtual screening against decoys, pose prediction of known actives, and prediction of binding affinity from crystal structures. Although the summary of the results is still in preparation, by almost all measures they were somewhat discouraging, with correlations to predictions using various physically based methods significantly worse than 1 kcal/mol

root-mean-square error. Interestingly, the best method was a less computationally demanding approximation to MM-PBSA that essentially ignored the entropy contribution<sup>237</sup> but even this method was very unreliable. The initial SAMPL generated significant participation and interest and is very likely to continue.

In the foreseeable future, fully atomistic free-energy calculations may be most important not solely for reliable predictions of binding affinity, but for a wealth of additional atomistic information such as probabilities of occupation of binding pose and water structure in the binding site that are impossible to gather from either experiment or more approximate methods. Free-energy calculations may also be of use in the future for the computation of octanol/water partition coefficients of molecules that are difficult to predict by standard rule-based algorithms like CLOGP or for even more direct membrane permeability simulations. Calculating the free energy, and thus stability, of different tautomers represents another important application of fully physical simulations. Questions of ligand-binding specificity can frequently be seen as a multivariate optimization problem, with binding to the intended target maximized, while binding to the alternative targets is minimized.

For further information, readers are encouraged to read a number of reviews on the subject of free-energy calculations published more recently,<sup>8-11,13,238-240</sup> useful textbooks,<sup>15-17,231</sup> as well as older reviews and books that may provide more historical perspective.<sup>32,241,242</sup>

A number of the reviews on the subject of free-energy calculations in ligand binding since the late 1980s conclude that free-energy calculations of ligand binding have finally overcome the problems and false starts of the past and that the time for free energies in pharmaceutical industry is nearly here or has already arrived. We will not make nearly as strong a claim here. An extensive survey of the latest results is somewhat mixed, and it is not clear that these methods will necessarily be an important part of the pharmaceutical work flow anytime in the near future. In some cases, computational simulations may be approaching the level of accuracy that they can provide some additional utility in some aspects of lead optimization, but the accuracy and speed of the methods presented in this chapter must both be improved drastically. Many computational chemists working in industry that were questioned by the authors thought that rigorous free-energy methods may eventually become a routine part of drug discovery methods but perhaps not for another twenty years.

It does, however, appear that improvements in computational power and methodologies have made it possible to compute increasingly reliable relative and absolute binding affinities, albeit with significant computational and human effort. Continuing improvements in techniques will make physics-based simulations more and more attractive, leading to improved simulation tools and eventually to a vital place in the pharmaceutical work flow.

## REFERENCES

- Houston, J. G.; Banks, M. N.; Binnie, A.; Brenner, S.; O'Connell, J.; Petrillo, E. W. Case study: impact of technology investment on lead discovery at Bristol Myers Squibb, 1998–2006. *Drug Discov. Today* **2008**, *13*, 44–51.
- Keseru, G. M.; Makara, G. M. Hit discovery and hit-to-lead approaches. *Drug Discov. Today* **2006**, *11*, 741–748.
- Koppitz, M.; Eis, K. Automated medicinal chemistry. *Drug Discov. Today* **2006**, *11*, 561–568.
- Perola, E.; Walters, W.; Charifson, P. S. A detailed comparison of current docking and scoring methods on systems of pharmaceutical relevance. *Proteins* **2004**, *56*, 235–249.
- Warren, G. L.; Andrews, C. W.; Capelli, A.-M.; Clarke, B.; LaLonde, J.; Lambert, M. H.; Lindvall, M.; Nevins, N.; Semus, S. F.; Sender, S.; Tedesco, G.; Wall, I. D.; Woolven, J. M.; Peishoff, C. E.; Head, M. S. A critical assessment of docking programs and scoring functions. *J. Med. Chem.* **2006**, *49*(20), 5912–5931.
- Enyedy, I.; Egan, W. Can we use docking and scoring for hit-to-lead optimization? *J. Comput. Aided Mol. Des.* **2008**.
- Hajduk, P. J.; Sauer, D. R. Statistical analysis of the effects of common chemical substituents on ligand potency. *J. Med. Chem.* **2008**, *51*, 553–564.
- Shirts, M. R.; Mobley, D. L.; Chodera, J. D. Alchemical free energy calculations: ready for prime time? *Annu. Rep. Comput. Chem.* **2007**, *3*, 41–59.
- Huang, N.; Jacobson, M. P. Physics-based methods for studying protein-ligand interactions. *Curr. Opin. Drug Di. De.* **2007**, *10*, 325–331.
- Gilson, M. K.; Zhou, H.-X. Calculation of protein-ligand binding affinities. *Annu. Rev. Biophys. Biomed.* **2007**, *36*, 21–42.
- Meirovitch, H. Recent developments in methodologies for calculating the entropy and free energy of biological systems by computer simulation. *Curr. Opin. Struc. Biol.* **2007**, *17*, 181–186.
- Ytreberg, F. M.; Swendsen, R. H.; Zuckerman, D. M. Comparison of free energy methods for molecular systems. *J. Chem. Phys.* **2006**, *125*, 184114.
- Rodinger, T.; Pomès, R. Enhancing the accuracy, the efficiency and the scope of free energy simulations. *Curr. Opin. Struc. Biol.* **2005**, *15*, 164–170.
- Brandsdal, B. O.; Österberg, F.; Almlöf, M.; Feierberg, I.; Luzhkov, V. B.; Åqvist, J. Free energy calculations and ligand binding. *Adv. Prot. Chem.* **2003**, *66*, 123–158.
- Chipot, C.; Pohorille, A.; Eds. *Free Energy Calculations: Theory and Applications in Chemistry and Biology*, Vol. 86. New York: Springer, **2007**.
- Frenkel, D.; Smit, B. *Understanding Molecular Simulation: from Algorithms to Applications*. San Diego, CA: Academic Press; **2002**.
- Leach, A. R. *Molecular Modelling: Principles and Applications*. Harlow, Essex, England: Addison Wesley Longman Limited; **1996**.
- Allen, M. P.; Tildesley, D. J. *Computer Simulation of Liquids*. New York: Oxford University Press; **1987**.
- Woods, C. J.; Manby, F. R.; Mulholland, A. J. An efficient method for the calculation of quantum mechanics/molecular mechanics free energies. *J. Chem. Phys.* **2008**, *128*(1), 014109.
- Kollman, P. A.; Massova, I.; Reyes, C.; Kuhn, B.; Huo, S.; Chong, L.; Lee, M.; Lee, T.; Duan, Y.; Wang, W.; Donini, O.; Cieplak, P.; Srinivasan, J.; Case, D. A.; Cheatham, T. E. Calculating structures and free energies of complex molecules: combining molecular mechanics and continuum models. *Acc. Chem. Res.* **2000**, *33*, 889–897.
- Lee, M. S.; Olson, M. A. Calculation of absolute protein-ligand binding affinity using path and endpoint approaches. *Biophys J.* **2006**, *90*, 864–877.
- Gohlke, H.; Case, D. A. Converging free energy estimates: Mm-pb(gb)sa studies on the protein-protein complex ras-raf. *J. Comput. Chem.* **2004**, *25*, 238–250.
- Swanson, J. M. J.; Henchman, R. H.; McCammon, J. A. Revisiting free energy calculations: a theoretical connection to MM/PBSA and direct calculation of the association free energy. *Biophys J.* **2004**, *86*, 67–74.
- Daggett, V. Long timescale simulations. *Curr. Opin. Struc. Biol.* **2000**, *10*, 160–164.
- Sitkoff, D.; Sharp, K.; Honig, B. H. Accurate calculation of hydration free energies using macroscopic solvent models. *J. Phys. Chem.* **1994**, *98*, 1978–1988.
- Honig, B. H.; Nicholls, A. Classical electrostatics in biology and chemistry. *Science* **1995**, *268*, 1144–1149.
- Gilson, M. K.; Sharp, K.; Honig, B. H. Calculating the electrostatic potential of molecules in solution: method and error assessment. *J. Comput. Chem.* **1987**, *9*, 327–335.
- Gilson, M. K.; Honig, B. H. Calculation of the total electrostatic energy of a macromolecular system: solvation energies, binding energies, and conformational analysis. *Proteins* **1988**, *4*, 7–18.
- Rubinstein, A.; Sherman, S. Influence of the solvent structure on the electrostatic interactions in proteins. *Biophys J.* **2004**, *87*, 1544–1557.
- Swanson, J. M. J.; Mongan, J.; McCammon, J. A. Limitations of atom-centered dielectric functions in implicit solvent models. *J. Phys. Chem. B* **2005**, *109*, 14769–14772.
- Schutz, C. N.; Warshel, A. What are the dielectric “constants” of proteins and how to validate electrostatic models? *Proteins* **2001**, *44*, 400–417.
- Archontis, G.; Simonson, T.; Karplus, M. Binding free energies and free energy components from molecular dynamics and Poisson-Boltzmann calculations: Application to amino acid recognition by aspartyl-tRNA. *J. Mol. Biol.* **2001**, *306*, 307–327.
- Sharp, K.; Honig, B. H. Electrostatic interactions in macromolecules: theory and applications. *Annu. Rev. Biophys. Biol.* **1990**, *19*, 301–332.
- Richards, F. M. Areas, volumes, packing and protein structure. *Annu. Rev. Biophys. Biol.* **1977**, *6*, 151–176.
- Sharp, K.; Nicholls, A.; Fine, R. F.; Honig, B. H. Reconciling the magnitude of the microscopic and macroscopic hydrophobic effects. *Science* **1991**, *252*, 106–109.
- Hermann, R. B. Theory of hydrophobic bonding. II. The correlation of hydrocarbon solubility in water with solvent cavity surface area. *J. Phys. Chem.* **1972**, *76*, 2754–2759.
- Reynolds, J. A.; Gilbert, D. B.; Tanford, C. Empirical correlation between hydrophobic free energy and aqueous cavity surface area. *Proc. Natl. Acad. Sci. U.S.A.* **1974**, *71*, 2925–2927.
- Gallicchio, E.; Kubo, M. M.; Levy, R. M. Enthalpy-entropy and cavity decomposition of alkane hydration free energies: Numerical results and implications for theories of hydrophobic solvation. *J. Phys. Chem. B* **2000**, *104*, 6271–6285.
- Wagoner, J. A.; Baker, N. A. Assessing implicit models for nonpolar mean solvation forces: the importance of dispersion and volume terms. *P. Natl. Acad. Sci. U.S.A.* **2006**, *103*, 8331–8336.
- Tan, C.; Tan, Y.-H.; Luo, R. Implicit nonpolar solvent models. *J. Phys. Chem. B* **2007**, *111*, 12263–12274.
- Levy, R. M.; Zhang, L. Y.; Gallicchio, E.; Felts, T. On the nonpolar hydration free energy of proteins: surface area and

- continuum solvent models for the solute-solvent interaction energy. *J. Am. Chem. Soc.* **2003**, *125*, 9523–9530.
42. Luo, H.; Sharp, K. On the calculation of absolute macromolecular binding free energies. *Proc. Natl. Acad. Sci. U.S.A.* **2002**, *99*, 10399–10404.
43. Brooks, B. R.; Janezic, D.; Karplus, M. Harmonic analysis of large systems. I. Methodology. *J. Comput. Chem.* **2004**, *16*, 1522–1542.
44. Bohm, H. J. The development of a simple empirical scoring function to estimate the binding constant for a protein-ligand complex of known three-dimensional structure. *J. Comput. Aid. Mol. Des.* **1994**, *8*, 243–256.
45. Hnizdo, V.; Tan, J.; Killian, B. J.; Gilson, M. K. Efficient calculation of configurational entropy from molecular simulations by combining the mutual-information expansion and nearest-neighbor methods. *J. Comput. Chem.* **2008**, *29*(10), 1605–1614.
46. Froloff, N.; Windemuth, A.; Honig, B. H. On the calculation of binding free energies using continuum methods: application to MHC class I protein-peptide interactions. *Protein Sci.* **1997**, *6*, 1293–301.
47. Hünenberger, P. H.; Helms, V.; Narayana, N.; Taylor, S. S.; McCammon, J. A. Determinants of ligand binding to camp-dependent protein kinase. *Biochemistry* **1999**, *38*, 2358–2366.
48. Jian Shen, J. W. Electrostatic binding energy calculation using the finite difference solution to the linearized Poisson-Boltzmann equation: assessment of its accuracy. *J. Comput. Chem.* **1996**, *17*, 350–357.
49. Schapira, M.; Torrv, M. Prediction of the binding energy for small molecules, peptides and proteins. *J. Mol. Recognit.* **1999**, *12*, 177–190.
50. Mobley, D. L.; Dill, K. A.; Chodera, J. D. Treating entropy and conformational changes in implicit solvent simulations of small molecules. *J. Phys. Chem. B* **2008**, *112*, 938–946.
51. Olson, M. A. Modeling loop reorganization free energies of acetylcholinesterase: a comparison of explicit and implicit solvent models. *Proteins* **2004**, *57*, 645–650.
52. Brown, S. P.; Muchmore, S. W. High-throughput calculation of protein-ligand binding affinities: modification and adaptation of the MM-PBSA protocol to enterprise grid computing. *J. Chem. Inf. Model.* **2006**, *46*, 999–1005.
53. Bashford, D.; Case, D. A. Generalized born models of macromolecular solvation effects. *Annu. Rev. Phys. Chem.* **2000**, *51*, 129–152.
54. Onufriev, A.; Bashford, D.; Case, D. A. Modification of the generalized Born model suitable for macromolecules. *J. Phys. Chem. B* **2000**, *104*, 3712–3720.
55. Onufriev, A.; Case, D. A.; Bashford, D. Effective Born radii in the generalized Born approximation: the importance of being perfect. *J. Comput. Chem.* **2002**, *23*, 1297–1304.
56. Feig, M.; Onufriev, A.; Lee, M. S.; Im, W.; Case, D. A.; Brooks, C. L., III. Performance comparison of generalized Born and Poisson methods in the calculation of electrostatic solvation energies for protein structures. *J. Comput. Chem.* **2004**, *25*, 265–284.
57. Geney, R.; Layten, M.; Gomperts, R.; Hornak, V.; Simmerling, C. Investigation of salt bridge stability in a generalized born solvent model. *J. Chem. Theory Comput.* **2006**, *2*, 115–127.
58. Nymeyer, H.; Garcia, A. E. Simulation of the folding equilibrium of alpha-helical peptides: a comparison of the generalized born approximation with explicit solvent. *Proc. Natl. Acad. Sci. U.S.A.* **2003**, *100*, 13934–13939.
59. Gilson, M. K.; Honig, B. H. The inclusion of electrostatic hydration energies in molecular mechanics calculations. *J. Comput. Aid. Mol. Des.* **1991**, *5*, 5–20.
60. Head, M. S.; Given, J. A.; Gilson, M. K. “Mining Minima”: direct computation of conformational free energy. *J. Phys. Chem. A* **1997**, *101*, 1609–1618.
61. Kolossváry, I. Evaluation of the molecular configuration integral in all degrees of freedom for the direct calculation of conformational free energies: prediction of the anomeric free energy of monosaccharides. *J. Phys. Chem. A* **1997**, *101*(51), 9900–9905.
62. Ragusa, A.; Hayes, J. M.; Light, M. E.; Kilburn, J. D. Predicting enantioselectivity: computation as an efficient experimental tool for probing enantioselectivity. *Eur. J. Org. Chem.* **2006**, *2006*(9), 3545–3549.
63. Ragusa, A.; Hayes, J. M.; Light, M. E.; Kilburn, J. D. A combined computational and experimental approach for the analysis of the enantioselective potential of a new macrocyclic receptor for n-protected  $\alpha$ -amino acids. *Chem. Eur. J.* **2007**, *13*(9), 2717–2728.
64. Potter, M. J.; Gilson, M. K. Coordinate systems and the calculation of molecular properties. *J. Phys. Chem. A* **2002**, *106*(3), 563–566.
65. Chang, C.-E. A.; Gilson, M. K. Free energy, entropy, and induced fit in host-guest recognition: calculations with the second-generation mining minima algorithm. *J. Am. Chem. Soc.* **2004**, *126*(40), 13156–13164.
66. Chang, C.-E.; Chen, W.; Gilson, M. K. Calculation of cyclodextrin binding affinities: energy, entropy, and implications for drug design. *Biophys. J.* **2004**, *87*, 3035–3049.
67. Chen, W.; Chang, C.-E. A.; Gilson, M. K. Concepts in receptor optimization: Targeting the rgd peptide. *J. Am. Chem. Soc.* **2006**, *128*(14), 4675–4684.
68. Chang, C.-E. A.; Chen, W.; Gilson, M. K. Ligand configurational entropy and protein binding. *Proc. Natl. Acad. Sci. U.S.A.* **2007**, *104*(5), 1534–1539.
69. Killian, B. J.; Yundenfreund Kravitz, J.; Gilson, M. K. Extraction of configurational entropy from molecular simulations via an expansion approximation. *J. Chem. Phys.* **2007**, *127*(2), 024107.
70. Chang, C.-E. A.; Chen, W.; Gilson, M. K. Evaluating the accuracy of the quasiharmonic approximation. *J. Chem. Theory Comput.* **2005**, *1*(5), 1017–1028.
71. Young, T.; Abel, R.; Kim, B.; Berne, B. J.; Friesner, R. A. Motifs for molecular recognition exploiting hydrophobic enclosure in protein-ligand binding. *Proc. Natl. Acad. Sci. U.S.A.* **2007**, *104*, 808–813.
72. Zwanzig, R. W. High-temperature equation of state by a perturbation method. I. Nonpolar gases. *J. Chem. Phys.* **1954**, *22*(8), 1420–1426.
73. Shirts, M. R.; Pande, V. S. Comparison of efficiency and bias of free energies computed by exponential averaging, the bennett acceptance ratio, and thermodynamic integration. *J. Chem. Phys.* **2005**, *122*, 144107.
74. Lu, N. D.; Singh, J. K.; Kofke, D. A. Appropriate methods to combine forward and reverse free-energy perturbation averages. *J. Chem. Phys.* **2003**, *118*(7), 2977–2984.
75. Wu, D.; Kofke, D. A. Asymmetric bias in free-energy perturbation measurements using two Hamiltonian-based models. *Phys. Rev. E* **2005**, *70*, 066702.
76. Jarzynski, C. Rare events and the convergence of exponentially averaged work values. *Phys. Rev. E* **2006**, *73*, 046105.
77. Widom, B. Some topics in the theory of fluids. *J. Chem. Phys.* **1963**, *39*(11), 2808–2812.
78. Jorgensen, W. L.; Ravimohan, C. Monte Carlo simulation of differences in free energies of hydration. *J. Chem. Phys.* **1985**, *83*(6), 3050–3054.

79. Resat, H.; Mezei, M. Studies on free energy calculations. I. Thermodynamic integration using a polynomial path. *J. Chem. Phys.* **1993**, *99*(8), 6052–6061.
80. Pitera, J. W.; van Gunsteren, W. F. A comparison of non-bonded scaling approaches for free energy calculations. *Mol. Simulat.* **2002**, *28*(1–2), 45–65.
81. Shirts, M. R.; Pitera, J. W.; Swope, W. C.; Pande, V. S. Extremely precise free energy calculations of amino acid side chain analogs: comparison of common molecular mechanics force fields for proteins. *J. Chem. Phys.* **2003**, *119*(11), 5740–5761.
82. Beutler, T. C.; Mark, A. E.; van Schaik, R. C.; Gerber, P. R.; van Gunsteren, W. F. Avoiding singularities and numerical instabilities in free energy calculations based on molecular simulations. *Chem. Phys. Lett.* **1994**, *222*, 529–539.
83. Mobley, D. L. Unpublished data.
84. Pearlman, D. A.; Kollman, P. A. The lag between the Hamiltonian and the system configuration in free-energy perturbation calculations. *J. Chem. Phys.* **1989**, *91*(12), 7831–7839.
85. Hendrix, D. A.; Jarzynski, C. A “fast growth” method of computing free energy differences. *J. Chem. Phys.* **2001**, *114*(14), 5974–5961.
86. Oostenbrink, C.; van Gunsteren, W. F. Calculating zeros: nonequilibrium free energy calculations. *Chem. Phys.* **2006**, *323*, 102–108.
87. Oostenbrink, C.; van Gunsteren, W. F. Free energies of ligand binding for structurally diverse compounds. *Proc. Natl. Acad. Sci. U.S.A.* **2005**, *102*(19), 6750–6754.
88. Crooks, G. E. Path-ensemble averages in systems driven far from equilibrium. *Phys. Rev. E* **2000**, *61*(3), 2361–2366.
89. Bennett, C. H. Efficient estimation of free energy differences from Monte Carlo data. *J. Comput. Phys.* **1976**, *22*, 245–268.
90. Shirts, M. R.; Bair, E.; Hooker, G.; Pande, V. S. Equilibrium free energies from nonequilibrium measurements using maximum-likelihood methods. *Phys. Rev. Lett.* **2003**, *91*(14), 140601.
91. Rick, S. W. Increasing the efficiency of free energy calculations using parallel tempering and histogram reweighting. *J. Chem. Theory Comput.* **2006**, *2*, 939–946.
92. Ferrenberg, A. M.; Swendsen, R. H. Optimized Monte Carlo data analysis. *Phys. Rev. Lett.* **1989**, *63*(12), 1195–1198.
93. Kumar, S.; Bouzida, D.; Swendsen, R. H.; Kollman, P. A.; Rosenberg, J. M. The weighted histogram analysis method for free-energy calculations on biomolecules. I. The method. *J. Comput. Chem.* **1992**, *13*(8), 1011–1021.
94. Bartels, C.; Karplus, M. Multidimensional adaptive umbrella sampling: applications to main chain and side chain peptide conformations. *J. Comput. Chem.* **1997**, *18*(12), 1450–1462.
95. Gallicchio, E.; Andrec, M.; Felts, A. K.; Levy, R. M. Temperature weighted histogram analysis method, replica exchange, and transition paths. *J. Phys. Chem. B* **2005**, *109*, 6722–6731.
96. Souaille, M.; Roux, B. Extension to the weighted histogram analysis method: combining umbrella sampling with free energy calculations. *Comput. Phys. Commun.* **2001**, *135*(1), 40–57.
97. Wang, J.; Deng, Y.; Roux, B. Absolute binding free energy calculations using molecular dynamics simulations with restraining potentials. *Biophys. J.* **2006**, *91*, 2798–2814.
98. Shirts, M. R.; Chodera, J. D. Statistically optimal analysis of samples from multiple equilibrium states. *J. Chem. Phys.* **2008**, *129*, 129105.
99. Steinbrecher, T.; Mobley, D. L.; Case, D. A. Nonlinear scaling schemes for Lennard-Jones interactions in free energy calculations. *J. Chem. Phys.* **2007**, *127*(21).
100. Pearlman, D. A.; Connelly, P. R. Determination of the differential effects of hydrogen bonding and water release on the binding of FK506 to native and TYR82 → PHE82 FKBP-12 proteins using free energy simulations. *J. Mol. Biol.* **1995**, *248*(3), 696–717.
101. Wang, L.; Hermans, J. Change of bond length in free-energy simulations: algorithmic improvements, but when is it necessary? *J. Chem. Phys.* **1994**, *100*(12), 9129–9139.
102. Boreesch, S.; Karplus, M. The Jacobian factor in free energy simulations. *J. Chem. Phys.* **1996**, *105*(12), 5145–5154.
103. Zacharias, M.; Straatsma, T. P.; McCammon, J. A. Separation-shifted scaling, a new scaling method for Lennard-Jones interactions in thermodynamic integration. *J. Phys. Chem.* **1994**, *100*(12), 9025–9031.
104. Shirts, M. R.; Pande, V. S. Solvation free energies of amino acid side chains for common molecular mechanics water models. *J. Chem. Phys.* **2005**, *122*, 134508.
105. Blondel, A. Ensemble variance in free energy calculations by thermodynamic integration: theory, optimal alchemical path, and practical solutions. *J. Comput. Chem.* **2004**, *25*(7), 985–993.
106. Rödinger, T.; Howell, P. L.; Pomès, R. Absolute free energy calculations by thermodynamic integration in four spatial dimensions. *J. Chem. Phys.* **2005**, *123*, 034104.
107. Lee, M. S.; Olson, M. A. Calculation of absolute protein-ligand binding affinity using path and endpoint approaches. *Biophys. J.* **2006**, *90*, 864–877.
108. Woo, H.-J.; Roux, B. Calculation of absolute protein-ligand binding free energy from computer simulation. *Proc. Natl. Acad. Sci. U.S.A.* **2005**, *102*, 6825–6830.
109. Ytreberg, F. M. Absolute FKBP binding affinities obtained by nonequilibrium unbinding simulations. *J. Chem. Phys.* **2009**, *130*, 164906-8.
110. Gan, W.; Roux, B. Binding specificity of SH2 domains: insight from free energy simulations. *Proteins* **2008**, *74*, 996–1007.
111. Torrie, G. M.; Valleau, J. P. Non-physical sampling distributions in Monte-Carlo free-energy estimation: umbrella sampling. *J. Comput. Phys.* **1977**, *23*(2), 187–199.
112. Mobley, D. L.; Chodera, J. D.; Dill, K. A. Confine-and-release method: obtaining correct binding free energies in the presence of protein conformational change. *J. Chem. Theory Comput.* **2007**, *3*(4), 1231–1235.
113. Mobley, D. L.; Graves, A. P.; Chodera, J. D.; McReynolds, A. C.; Shoichet, B. K.; Dill, K. A. Predicting absolute ligand binding free energies to a simple model site. *J. Mol. Biol.* **2007**, *371*(4), 1118–1134.
114. Okamoto, Y. Generalized-ensemble algorithms: enhanced sampling techniques for Monte Carlo and molecular dynamics simulations. *J. Mol. Graph. Model.* **2004**, *22*, 425–439.
115. Pitera, J. W.; Kollman, P. A. Exhaustive mutagenesis in silico: multicoordinate free energy calculations in proteins and peptides. *Proteins* **2000**, *41*, 385–397.
116. Roux, B.; Faraldo-Gómez, J. D. Characterization of conformational equilibria through Hamiltonian and temperature replica-exchange simulations: assessing entropic and environmental effects. *J. Comput. Chem.* **2007**, *28*(10), 1634–1647.
117. Woods, C. J.; Essex, J. W.; King, M. A. Enhanced configurational sampling in binding free energy calculations. *J. Phys. Chem. B* **2003**, *107*, 13711–13718.
118. Banba, S.; Guo, Z.; Brooks, C. L., III. Efficient sampling of ligand orientations and conformations in free energy calculations using the lambda-dynamics method. *J. Phys. Chem. B* **2000**, *104*(29), 6903–6910.

119. Bitetti-Putzer, R.; Yang, W.; Karplus, M. Generalized ensembles serve to improve the convergence of free energy simulations. *Chem. Phys. Lett.* **2003**, *377*, 633–641.
120. Hritz, J.; Oostenbrink, C. Hamiltonian replica exchange molecular dynamics using soft-core interactions. *J. Chem. Phys.* **2008**, *128*(14), 144121.
121. Guo, Z.; Brooks, C. L., III; Kong, X. Efficient and flexible algorithm for free energy calculations using the  $\lambda$ -dynamics approach. *J. Phys. Chem. B* **1998**, *102*, 2032–2036.
122. Kong, X.; Brooks, C. L., III.  $\lambda$ -dynamics: a new approach to free energy calculations. *J. Chem. Phys.* **1996**, *105*(6), 2414–2423.
123. Li, H.; Fajer, M.; Yang, W. Simulated scaling method for localized enhanced sampling and simultaneous “alchemical” free energy simulations: a general method for molecular mechanical, quantum mechanical, and quantum mechanical/molecular mechanical simulations. *J. Chem. Phys.* **2007**, *126*, 024106.
124. Zheng, L.; Carbone, I. O.; Lugovskoy, A.; Berg, B. A.; Yang, W. A hybrid recursion method to robustly ensure convergence efficiencies in the simulated scaling based free energy simulations. *J. Chem. Phys.* **2008**, *129*(3), 034105.
125. Zheng, L.; Yang, W. Essential energy space random walks to accelerate molecular dynamics simulations: convergence improvements via an adaptive-length self-healing strategy. *J. Chem. Phys.* **2008**, *129*(1), 014105.
126. Min, D.; Yang, W. Energy difference space random walk to achieve fast free energy calculations. *J. Chem. Phys.* **2008**, *128*(19).
127. Li, H.; Yang, W. Forging the missing link in free energy estimations: lambda-WHAM in thermodynamic integration, overlap histogramming, and free energy perturbation. *Chem. Phys. Lett.* **2007**, *440*(1–3), 155–159.
128. Min, D.; Li, H.; Li, G.; Bitetti-Putzer, R.; Yang, W. Synergistic approach to improve “alchemical” free energy calculation in rugged energy surface. *J. Chem. Phys.* **2007**, *126*(14), 144109.
129. Oostenbrink, C.; van Gunsteren, W. F. Free energies of binding of polychlorinated biphenyls to the estrogen receptor from a single simulation. *Proteins* **2004**, *54*(2), 237–246.
130. Oostenbrink, C.; van Gunsteren, W. F. Single-step perturbations to calculate free energy differences from unphysical reference states: limits on size, flexibility, and character. *J. Comput. Chem.* **2003**, *24*(14), 1730–1739.
131. Schwab, E.; van Gunsteren, W. F.; Zagrovic, B. Computational study of the mechanism and the relative free energies of binding of anticholesteremic inhibitors to squalene-hopene cyclase. *Biochemistry* **2008**, *47*(9), 2945–2951.
132. Srinivasan, J. III; Cheatham, T. E.; Cieplak, P.; Kollman, P. A.; Case, D. A. Continuum solvent studies of the stability of DNA, RNA, and phosphoramidate-DNA helices. *J. Am. Chem. Soc.* **1998**, *120*, 9401–9409.
133. Cheatham, T. E.; Srinivasan, J.; Case, D. A.; Kollman, P. A. Molecular dynamics and continuum solvent studies of the stability of polyG-polyC and polyA-polyT DNA duplexes in solution. *J. Biomol. Struct. Dyn.* **1998**, *16*, 265–280.
134. Chong, L.; Duan, Y.; Wang, L.; Massova, I.; Kollman, P. A. Molecular dynamics and free-energy calculations applied to affinity maturation in antibody 48g7. *Proc. Natl. Acad. Sci. U.S.A.* **1995**, *96*, 14330–14335.
135. Foloppe, N.; Fisher, L. M.; Howes, R.; Kierstan, P.; Potter, A.; Robertson, A. G.; Surgenor, A. E. Structure-based design of novel CHK1 inhibitors: insights into hydrogen bonding and protein-ligand affinity. *J. Med. Chem.* **2005**, *48*, 4332–4345.
136. Bryce, R. A.; Hillier, I. H.; Naismith, J. H. Carbohydrate-protein recognition: molecular dynamics simulations and free energy analysis of oligosaccharide binding to concanavalin a. *Biophys. J.* **2001**, *81*, 1373–1388.
137. Kuhn, B.; Kollman, P. A.; Stahl, M. Prediction of pKa shifts in proteins using a combination of molecular mechanical and continuum solvent calculations. *J. Comput. Chem.* **2004**, *25*, 1865–1872.
138. Ferrara, P.; Gohlke, H.; Price, D. J.; Klebe, G.; Brooks, C. L., III. Assessing scoring functions for protein-ligand interactions. *J. Med. Chem.* **2004**, *47*, 3032–3047.
139. Massova, I.; Kollman, P. A. Computational alanine scanning to probe protein-protein interactions: a novel approach to evaluate binding free energies. *J. Am. Chem. Soc.* **1999**, *121*, 8133–8143.
140. Kuhn, B.; Kollman, P. A. A ligand that is predicted to bind better to avidin than biotin: insights from computational fluorine scanning. *J. Am. Chem. Soc.* **2000**, *122*, 3909–3916.
141. Kuhn, B.; Kollman, P. A. Binding of a diverse set of ligands to avidin and streptavidin: an accurate quantitative prediction of their relative affinities by a combination of molecular mechanics and continuum solvent models. *J. Med. Chem.* **2000**, *43*, 3786–3791.
142. Huo, S.; Wang, J.; Cieplak, P.; Kollman, P. A.; Kuntz, I. D. Molecular dynamics and free energy analyses of cathepsin d-inhibitor interactions: insight into structure-based ligand design. *J. Med. Chem.* **2002**, *45*, 1412–1419.
143. Mardis, K. L.; Luo, R.; Gilson, M. K. Interpreting trends in the binding of cyclic ureas to HIV-1 protease. *J. Mol. Biol.* **2001**, *309*, 507–517.
144. Schwarzl, S. M.; Tschopp, T. B.; Smith, J. C.; Fischer, S. Can the calculation of ligand binding free energies be improved with continuum solvent electrostatics and an ideal-gas entropy correction? *J. Comput. Chem.* **2002**, *23*, 1143–1149.
145. Rizzo, R. C.; Toba, S.; Kuntz, I. D. A molecular basis for the selectivity of thiazole urea inhibitors with stromelysin-1 and gelatinase-A from generalized born molecular dynamics simulations. *J. Med. Chem.* **2004**, *47*, 3065–3074.
146. Brown, S. P.; Muchmore, S. W. Rapid estimation of relative protein-ligand binding affinities using a high-throughput version of MM-PBSA. *J. Chem. Inf. Model.* **2007**, *47*, 1493–1503.
147. Kuhn, B.; Gerber, P. R.; Schulz-Gasch, T.; Stahl, M. Validation and use of the MM-PBSA approach for drug discovery. *J. Med. Chem.* **2005**, *48*, 4040–4048.
148. Pearlman, D. A. Evaluating the molecular mechanics Poisson-Boltzmann surface area free energy method using a congeneric series of ligands to p38 map kinase. *J. Med. Chem.* **2005**, *48*, 7796–7807.
149. Weis, A.; Katebzadeh, K.; Söderhjelm, P.; Nilsson, I.; Ryde, U. Ligand affinities predicted with the MM/PBSA method: dependence on the simulation method and the force field. *J. Med. Chem.* **2006**, *49*, 6596–6606.
150. Rafi, S. B.; Cui, G.; Song, K.; Cheng, X.; Tonge, P. J.; Simmerling, C. Insight through molecular mechanics Poisson-Boltzmann surface area calculations into the binding affinity of triclosan and three analogues for FabI, the *E. Coli* enoyl reductase. *J. Med. Chem.* **2006**, *49*, 4574–4580.
151. Donini, O.; Kollman, P. A. Calculation and prediction of binding free energies for the matrix metalloproteinases. *J. Med. Chem.* **2000**, *43*, 4180–4188.
152. Tembe, B. L.; McCammon, J. A. Ligand-receptor interactions. *Comput. Chem.* **1984**, *8*(4), 281–284.

153. Wong, C. F.; McCammon, J. A. Dynamics and design of enzymes and inhibitors. *J. Am. Chem. Soc.* **1986**, *108*(13), 3830–3832.
154. Hermans, J.; Subramaniam, S. The free energy of xenon binding to myoglobin from molecular dynamics simulation. *Israel J. Chem.* **1986**, *27*, 225–227.
155. Pearlman, D. A. Free energy calculations: methods for estimating ligand binding affinities. In: *Free Energy Calculations in Rational Drug Design*, Rami Reddy, M.; Erion, M. D.; Eds. Academic/Plenum; New York, NY: Kluwer, **2001**.
156. Chipot, C. Free energy calculations in biomolecular simulations: how useful are they in practice? In: *Lecture Notes in Computational Science and Engineering: New Algorithms for Molecular Simulation*, Leimkuhler, B.; Chipot, C.; Elber, R.; Laaksonen, A.; Mark, A. E.; Schlick, T.; Schütte, C.; Skeel, R.; Eds. Vol. 49. New York: Springer, **2005**, 183–209.
157. Rizzo, R. C.; Wang, D. P.; Tirado-Rives, J.; Jorgensen, W. L. Validation of a model for the complex of HIV-1 reverse transcriptase with sustiva through computation of resistance profiles. *J. Am. Chem. Soc.* **2000**, *122*(51), 12898–12900.
158. Wang, D.-P.; Rizzo, R. C.; Tirado-Rives, J.; Jorgensen, W. L. Antiviral drug design: computational analyses of the effects of the I100i mutation for HIV-RT on the binding of nrtis. *Bioorgan. Med. Chem. Lett.* **2001**, *11*(21), 2799–2802.
159. Udier-Blagovic, M.; Tirado-Rives, J.; Jorgensen, W. L. Structural and energetic analyses of the effects of the K103N mutation of HIV-1 reverse transcriptase on efavirenz analogues. *J. Med. Chem.* **2004**, *47*(9), 2389–2392.
160. Kim, J. T.; Hamilton, A. D.; Bailey, C. M.; Domoal, R. A.; Wang, L.; Anderson, K. S.; Jorgensen, W. L. Fep-guided selection of bicyclic heterocycles in lead optimization for non-nucleoside inhibitors of HIV-1 reverse transcriptase. *J. Am. Chem. Soc.* **2006**, *128*(48), 15372–15373.
161. Jorgensen, W. L.; Ruiz-Caro, J.; Tirado-Rives, J.; Basavathruni, A.; Anderson, K. S.; Hamilton, A. D. Computer-aided design of non-nucleoside inhibitors of HIV-1 reverse transcriptase. *Bioorg. Med. Chem. Lett.* **2006**, *16*(3), 663–667.
162. Kroeger Smith, M. B.; Rader, L. H.; Franklin, A. M.; Taylor, E. V.; Smith, K. D.; Tirado-Rives, J.; Jorgensen, W. L. Energetic effects for observed and unobserved HIV-1 reverse transcriptase mutations of residues I100, v106, and y181 in the presence of nevirapine and efavirenz. *Bioorg. Med. Chem. Lett.* **2008**, *18*(3), 969–972.
163. Zeevaart, J. G.; Wang, L.; Thakur, V. V.; Leung, C. S.; Tirado-Rives, J.; Bailey, C. M.; Domoal, R. A.; Anderson, K. S.; Jorgensen, W. L. Optimization of azoles as anti-human immunodeficiency virus agents guided by free-energy calculations. *J. Am. Chem. Soc.* **2008**, *120*, 9492–9499.
164. Henin, J.; Maignet, B.; Tarek, M.; Escrieut, C.; Fourmy, D.; Chipot, C. Probing a model of a GPCR/ligand complex in an explicit membrane environment: the human cholecystokinin-1 receptor. *Biophys. J.* **2006**, *90*(4), 1232–1240.
165. Yang, W.; Gao, Y. Q.; Cui, Q.; Ma, J.; Karplus, M. The missing link between thermodynamics and structure in fl-atpase. *Proc. Natl. Acad. Sci. U.S.A.* **2003**, *100*(3), 874–879.
166. Banerjee, A.; Yang, W.; Karplus, M.; Verdine, G. L. Structure of a repair enzyme interrogating undamaged DNA elucidates recognition of damaged DNA. *Nature* **2005** *434*, 612–618.
167. Oostenbrink, C.; Pitera, J. W.; van Lipzig, M. M. H.; Meerman, J. H. N.; van Gunsteren, W. F. Simulations of the estrogen receptor ligand-binding domain: affinity of natural ligands and xenoestrogens. *J. Med. Chem.* **2000**, *43*(24), 4594–4605.
168. Rami Reddy, M.; Erion, M. D. Calculation of relative binding free energy differences for fructose 1,6-bisphosphatase inhibitors using the thermodynamic cycle perturbation approach. *J. Am. Chem. Soc.* **2001**, *123*, 6246–6252.
169. Steinbrecher, T.; Case, D. A.; Labahn, A. A multistep approach to structure-based drug design: studying ligand binding at the human neutrophil elastase. *J. Med. Chem.* **2006**, *49*, 1837–1844.
170. Gouda, H.; Kuntz, I. D.; Case, D. A.; Kollman, P. A. Free energy calculations for theophylline binding to an RNA aptamer: comparison of MM-PBSA and thermodynamic integration methods. *Biopolymers* **2003**, *68*, 16–34.
171. Tanida, Y.; Ito, M.; Fujitani, H. Calculation of absolute free energy of binding for theophylline and its analogs to RNA aptamer using nonequilibrium work values. *Chem. Phys.* **2007**, *337*(1–3), 135–143.
172. Jiao, D.; Golubkov, P. A.; Darden, T. A.; Ren, P. Calculation of protein-ligand binding free energy using a polarizable potential. *Proc. Natl. Acad. Sci. U.S.A.* **2008**, *105*(17), 6290–6295.
173. Khoruzhii, O.; Donchev, A. G.; Galkin, N.; Illarionov, A.; Olevanov, M.; Ozrin, V.; Queen, C.; Tarasov, V. Application of a polarizable force field to calculations of relative protein-ligand binding affinities. *Proc. Natl. Acad. Sci. U.S.A.* **2008**, *105*(30), 10378–10383.
174. Price, D. J.; Jorgensen, W. L. Improved convergence of binding affinities with free energy perturbation: application to non-peptide ligands with pp60src SH2 domain. *J. Comput. Aided. Mol. Des.* **2001**, *15*, 681–695.
175. Fowler, P. W.; Jha, S.; Coveney, P. V. Grid-based steered thermodynamic integration accelerates the calculation of binding free energies. *Philos. T. R. Soc. B.* **2005**, *363*, 1999–2015.
176. Chipot, C.; Rozanska, X.; Dixit, S. B. Can free energy calculations be fast and accurate at the same time? Binding of low-affinity, non-peptide inhibitors to the SH2 domain of the src protein. *J. Comput. Aided Mol. Des.* **2005**, *19*, 765–770.
177. Fowler, P. W.; Gerout, S.; Jha, S.; Waksman, G.; Coveney, P. V. Rapid, accurate, and precise calculation of relative binding affinities for the SH2 domain using a computational grid. *J. Chem. Theory Comput.* **2007**, *3*(3), 1193–1202.
178. Pearlman, D. A.; Charifson, P. S. Are free energy calculations useful in practice? A comparison with rapid scoring functions for the p38 map kinase protein system. *J. Med. Chem.* **2001**, *44*, 3417–3423.
179. Mobley, D. L.; Chodera, J. D.; Dill, K. A. On the use of orientational restraints and symmetry corrections in alchemical free energy calculations. *J. Chem. Phys.* **2006**, *125*, 084902.
180. Gilson, M. K.; Given, J. A.; Bush, B. L.; McCammon, J. A. A statistical-thermodynamic basis for computation of binding affinities: a critical review. *Biophys. J.* **1997**, *72*(3), 1047–1069.
181. Deng, Y.; Roux, B. Computations of standard binding free energies with molecular dynamics simulations. *J. Phys. Chem. B* **2008**, in press.
182. Helms, V.; Wade, R. C. Hydration energy landscape of the active site cavity in cytochrome P450cam. *Proteins* **1998**, *32*(3), 381–396.
183. Helms, V.; Wade, R. C. Computational alchemy to calculate absolute protein-ligand binding free energy. *J. Am. Chem. Soc.* **1998**, *120*(12), 2710–2713.
184. Deng, Y.; Roux, B. Computation of binding free energy with molecular dynamics and grand canonical Monte Carlo simulations. *J. Chem. Phys.* **2008**, *128*(11).
185. Zhang, L.; Hermans, J. Hydrophilicity of cavities in proteins. *Proteins* **1996**, *24*(4), 433–438.

186. Olano, L. R.; Rick, S. W. Hydration free energies and entropies for water in protein interiors. *J. Am. Chem. Soc.* **2004**, *126*(25), 7991–8000.
187. Barillari, C.; Taylor, J.; Viner, R.; Essex, J. W. Classification of water molecules in protein binding sites. *J. Am. Chem. Soc.* **2007**, *129*(9), 2577–2587.
188. Hamelberg, D.; McCammon, J. A. Standard free energy of releasing a localized water molecule from the binding pockets of proteins: double-decoupling method. *J. Am. Chem. Soc.* **2004**, *126*, 7683–7689.
189. Lu, Y.; Wang, C.-Y.; Wang, S. Binding free energy contributions of interfacial waters in HIV-1 protease/inhibitor complexes. *J. Am. Chem. Soc.* **2006**, *128*, 11830–11839.
190. Roux, B.; Nina, M.; Pomès, R.; Smith, J. C. Thermodynamic stability of water molecules in the bacteriorhodopsin proton channel: a molecular dynamics free energy perturbation study. *Biophys. J.* **1996**, *71*(2), 670–681.
191. De Simone, A.; Dobson, G. G.; Verma, C. S.; Zagari, A.; Fraternali, F. Prion and water: tight and dynamical hydration sites have a key role in structural stability. *Proc. Natl. Acad. Sci. U.S.A.* **2005**, *102*(21), 7535–7540.
192. Pan, C.; Mezei, M.; Mujtaba, S.; Muller, M.; Zeng, L.; Li, J.; Wang, Z.; Zhou, M. M. Structure-guided optimization of small molecules inhibiting human immunodeficiency virus 1 tat association with the human coactivator p300/CREB binding protein-associated factor. *J. Med. Chem.* **2007**, *50*(10), 2285–2288.
193. Eriksson, A. E.; Baase, W. A.; Zhang, X. J.; Heinz, D. W.; Blaber, M.; Baldwin, E. P.; Matthews, B. W. Response of a protein structure to cavity-creating mutations and its relation to the hydrophobic effect. *Science* **1992**, *255*, 178–183.
194. Eriksson, A. E.; Baase, W. A.; Matthews, B. W. Similar hydrophobic replacements of leu99 and phe153 within the core of T4 lysozyme have different structural and thermodynamic consequences. *J. Mol. Biol.* **1993**, *229*, 747–769.
195. Morton, A.; Matthews, B. W. Specificity of ligand binding in a buried nonpolar cavity of T4 lysozyme: linkage of dynamics and structural plasticity. *Biochemistry* **1995**, *34*, 8576–8588.
196. Morton, A.; Baase, W. A.; Matthews, B. W. Energetic origins of specificity of ligand binding in an interior nonpolar cavity of T4 lysozyme. *Biochemistry* **1995**, *34*, 8564–8575.
197. Wei, B. Q.; Baase, W. A.; Weaver, L. H.; Matthews, B. W.; Shoichet, B. K. A model binding site for testing scoring functions in molecular docking. *J. Mol. Biol.* **2002**, *322*, 339–355.
198. Wei, B. Q.; Weaver, L. H.; Ferrari, A. M.; Matthews, B. W.; Shoichet, B. K. Testing a flexible-receptor docking algorithm in a model binding site. *J. Mol. Biol.* **2004**, *337*, 1161–1182.
199. Graves, A. P.; Brenk, R.; Shoichet, B. K. Decoys for docking. *J. Med. Chem.* **2005**, *48*, 3714–3728.
200. Hermans, J.; Wang, L. Inclusion of the loss of translational and rotational freedom in theoretical estimates of free energies of binding. Application to a complex of benzene and mutant T4 lysozyme. *J. Am. Chem. Soc.* **1997**, *119*, 2707–2714.
201. Mann, G.; Hermans, J. Modeling protein-small molecule interactions: structure and thermodynamics of noble gases binding in a cavity in mutant phage T4 lysozyme L99A. *J. Mol. Biol.* **2000**, *302*, 979–989.
202. Boresch, S.; Tettinger, F.; Leitgeb, M.; Karplus, M. Absolute binding free energies: a quantitative approach for their calculation. *J. Phys. Chem. A* **2003**, *107*(35), 9535–9551.
203. Deng, Y.; Roux, B. Calculation of standard binding free energies: aromatic molecules in the T4 lysozyme L99A mutant. *J. Chem. Theory Comput.* **2006**, *2*, 1255–1273.
204. Clark, M.; Guarnieri, F.; Shkurko, I.; Wiseman, J. Grand canonical Monte Carlo simulation of ligand-protein binding. *J. Chem. Info. Model.* **2006**, *46*(1), 231–242.
205. Mobley, D. L.; Dumont, È.; Chodera, J. D.; Dill, K. A. Comparison of charge models for fixed-charge force fields: small-molecule hydration free energies in explicit solvent. *J. Phys. Chem. B* **2007**, *111*(9), 2242–2254.
206. Holt, D. A.; Luengo, J. I.; Yamashita, D. S.; Oh, H. J.; Konialian, A. L.; Yen, H. K.; Rozamus, L. W.; Brandt, M.; Bossard, M. J.; Levy, M. A.; Eggleston, D. S.; Liang, J.; Schultz, L. W.; Stout, T. J.; Clardy, J. Design, synthesis, and kinetic evaluation of high-affinity FKBP ligands and the x-ray crystal structures of their complexes with FKBP12. *J. Am. Chem. Soc.* **1993**, *115*(22), 9925–9938.
207. Shirts, M. R. *Calculating precise and accurate free energies in biomolecular systems*. Ph.D. dissertation, Stanford, January **2005**.
208. Fujitani, H.; Tanida, Y.; Ito, M.; Shirts, M. R.; Jayachandran, G.; Snow, C. D.; Sorin E. J.; Pande, V. S. Direct calculation of the binding free energies of FKBP ligands. *J. Chem. Phys.* **2005**, *123*, 84–108.
209. Jayachandran, G.; Shirts, M. R.; Park, S.; Pande, V. S. Parallelized-over-parts computation of absolute binding free energy with docking and molecular dynamics. *J. Chem. Phys.* **2006**, *125*, 084901.
210. Dixit, S. B.; Chipot, C. Can absolute free energies of association be estimated from molecular mechanical simulations? The biotin-streptavidin system revisited. *J. Phys. Chem. A* **2001**, *105*(42), 9795–9799.
211. Hess, B.; van der Vegt, N. F. A. Hydration thermodynamic properties of amino acid analogues: a comparison of biomolecular force fields and water models. *J. Phys. Chem. B* **2006**, *110*, 17616–17626.
212. Nicholls, A.; Mobley, D. L.; Guthrie, P. J.; Chodera, J. D.; Pande, V. S. Predicting small-molecule solvation free energies: an informal blind test for computational chemistry. *J. Med. Chem.* **2008**, *51*, 769–779.
213. Steinbrecher, T.; Hrenn, A.; Dormann, K. L.; Merfort, I.; Labahn, A. Bornyl (3,4,5-trihydroxy)-cinnamate: an optimized human neutrophil elastase inhibitor designed by free energy calculations. *Bioorgan. Med. Chem.* **2008**, *16*(5), 2385–2390.
214. Talhout, R.; Villa, A.; Mark, A. E.; Engberts, J. B. Understanding binding affinity: a combined isothermal titration calorimetry/molecular dynamics study of the binding of a series of hydrophobically modified benzamidinium chloride inhibitors to trypsin. *J. Am. Chem. Soc.* **2003**, *125*(35), 10570–10579.
215. Mao, H. Z.; Weber, J. Identification of the betatp site in the x-ray structure of f1-atpase as the high-affinity catalytic site. *Proc. Natl. Acad. Sci. U.S.A.* **2007**, *104*(47), 18478–18483.
216. Zagrovic, B.; van Gunsteren, W. F. Computational analysis of the mechanism and thermodynamics of inhibition of phosphodiesterase 5a by synthetic ligands. *J. Chem. Theory Comput.* **2007**, *3*, 301–311.
217. Leitgeb, M.; Schröder, C.; Boresch, S. Alchemical free energy calculations and multiple conformational substates. *J. Chem. Phys.* **2005**, *122*, 084109.
218. de Graaf, C.; Oostenbrink, C.; Keizers, P. H. J.; van Vugt-Lussenburg, B. M. A.; Commandeur, J. N. M.; Vermeulen, N. P. E. Free energies of binding of R- and S- propranolol to wild-type and f483a mutant cytochrome p450 d26 from molecular dynamics simulations. *Eur. Biophys. J.* **2007**, *36*(6), 589–599.

219. van den Bosch, M.; Swart, M.; Snijders, J. G.; Berendsen, H. J. C.; Mark, A. E.; Oostenbrink, C.; van Gunsteren, W. F.; Canters, G. W. Calculation of the redox potential of the protein azurin and some mutants. *ChemBioChem* **2005**, *6*(4), 738–746.
220. Dolenc, J.; Oostenbrink, C.; Koller, J.; van Gunsteren, W. F. Molecular dynamics simulations and free energy calculations of netropsin and distamycin binding to an aaaa DNA binding site. *Nucleic Acids Res.* **2005**, *33*(2), 725–733.
221. Donnini, S.; Juffer, A. H. Calculations of affinities of peptides for proteins. *J. Comput. Chem.* **2004**, *25*, 393–411.
222. Oostenbrink, C.; Villa, A.; Mark, A. E.; van Gunsteren, W. F. A biomolecular force field based on the free enthalpy of hydration and solvation: the GROMOS force-field parameter sets 53a5 and 53a6. *J. Comput. Chem.* **2004**, *25*(13), 1656–1676.
223. Hornak, V.; Abel, R.; Okur, A.; Strockbine, B.; Roitberg, A. E.; Simmerling, C. Comparison of multiple amber force fields and development of improved protein backbone parameters. *Proteins* **2006**, *65*(3), 712–725.
224. Kaminski, G.; Friesner, R. A.; Rives, J.; Jorgensen, W. L. Evaluation and reparametrization of the opls-aa force field for proteins via comparison with accurate quantum chemical calculations on peptides. *J. Phys. Chem. B* **2001**, *105*(28), 6474–6487.
225. Wang, J.; Wolf, R. M.; Caldwell, J. W.; Kollman, P. A.; Case, D. A. Development and testing of a general amber force field. *J. Comput. Chem.* **2004**, *25*(9), 1157–1174.
226. Jakalian, A.; Bush, B. L.; Jack, D. B.; Bayly, C. I. Fast, efficient generation of high-quality atomic charges, AM1-BCC model. I. Method. *J. Comput. Chem.* **2000**, *21*(2), 132–146.
227. Jakalian, A.; Jack, D. B.; Bayly, C. I. Fast, efficient generation of high-quality atomic charges, AM1-BCC model. II. Parameterization and validation. *J. Comput. Chem.* **2002**, *23*(16), 1623–1641.
228. Ponder, J. W.; Case, D. A. Force fields for protein simulations, in *Advances in Protein Chemistry*, Dagget, V.; Ed. San Diego, CA: Academic Press **2003**, *66*, 27–86.
229. Michel, J.; Verdonk, M. L.; Essex, J. W. Protein-ligand binding free energy predictions by implicit solvent simulation: a tool for lead optimization? *J. Med. Chem.* **2006**, *49*, 7427–7439.
230. Li, L.; Dantzer, J. J.; Nowacki, J.; O'Callaghan, B. J.; Meroueh, S. O. PDBCAL: a comprehensive dataset for receptor-ligand interactions with three-dimensional structures and binding thermodynamics from isothermal titration calorimetry. *Chem. Bio. Drug Des.* **2008**, *71*(6), 529–532.
231. Rami Reddy, M.; Erion, M. D., Eds. *Free Energy Calculations in Rational Drug Design*. Amsterdam: Kluwer Academic, **2001**.
232. Marti-Renom, M. A.; Madhusudhan, M. S.; Fiser, A.; Rost, B.; Sali, A. Reliability of assessment of protein structure prediction methods. *Structure* **2002**, *10*(3), 435–440.
233. Méndez, R.; Leplae, R.; Lesink, M. F.; Wodak, S. J. Assessment of CAPRI predictions in rounds 3–5 shows progress in docking procedures. *Proteins* **2005**, *60*(2), 150–169.
234. Day, G.M.; Motherwell, W. D. S.; Ammon, H. L.; Boerrigter, S. X. M.; Della Valle, R. G.; Venuti, E.; Dzyabchenko, A.; Dunitz, J. D.; Schweizer, B.; van Eijck, B. P.; Erk, P.; Facelli, J. C.; Bazterra, V. E.; Ferraro, M. B.; Hofmann, D. W. M.; Leusen, F. J. J.; Liang, C.; Pantelides, C. C.; Karamertzanis, P. G.; Price, S. L.; Lewis, T. C.; Nowell, H.; Torrisi, A.; Scheraga, H. A.; Arnautova, Y. A.; Schmidt, M. U.; and Verwer, P. A third blind test of crystal structure prediction. *Acta Crystall. B-Struc.*, **2005**, *61*(5), 511–527.
235. Parker, C. N. McMaster University data-mining and docking competition: computational models on the catwalk. *J. Biomol. Screen.* **2005**, *10*(7), 647–648.
236. Villa, A.; Zangi, R.; Pieffet, G.; Mark, A. E. Sampling and convergence in free energy calculations of protein-ligand interactions: the binding of triphenoxypyridine derivatives to factor xa and trypsin. *J. Comput. Aided Mol. Des.* **2003**, *17*(10), 673–686.
237. Naim, M.; Bhat, S.; Rankin, K. N.; Dennis, S.; Chowdhury, S. F.; Siddiqi, I.; Drabik, P.; Sulea, T.; Bayly, C. I.; Jakalian, A.; Purisima, E. O. Solvated interaction energy (sie) for scoring protein-ligand binding affinities. I. Exploring the parameter space. *J. Chem. Info. Model.* **2007**, *47*(1), 122–133.
238. Jorgensen, W. L. The many roles of computation in drug discovery. *Science* **2004**, *303*(5665), 1813–1818.
239. Chipot, C.; Pearlman, D. A. Free energy calculations: the long and winding gilded road. *Mol. Simulat.* **2002**, *28*(1–2), 1–12.
240. Mobley, D. L.; Dill, K. A. Binding of small-molecule ligand to proteins. “What you see” is not always “what you get.” *Structure* **2009**, *17*, 489–498.
241. Kollman, P. A. Free energy calculations: applications to chemical and biochemical phenomena. *Chem. Rev.* **1993**, *7*, 2395–2417.
242. Jorgensen, W. L. Free energy calculations: a breakthrough for modeling organic chemistry in solution. *Accounts Chem. Res.* **1989**, *22*(5), 184–189.